Journal of Transport & Health 13 (2019) 41–62

Contents lists available at ScienceDirect

Journal of Transport & Health

journal homepage: www.elsevier.com/locate/jth

The effects of changing passenger weight on aircraft flight performance

Damien J. Melis[a,*], Jose M. Silva[a], Miguel A. Silvestre[b], Richard Yeun[a]

[a] School of Engineering, RMIT University, GPO Box 2476, Melbourne 3001, Victoria, Australia
[b] C-MAST– Universidade da Beira Interior (UBI), 6200-001, Covilhã, Portugal

A B S T R A C T

Background: Global demand for air travel is increasing. Concurrently, the average weight of global population has been rising in the past decades, and this trend is set to persist in the near future. These two issues converge to the inevitable problem of dealing with a combination of increasing passengers on aircraft and their corresponding weight. Most aircraft performance assumptions rely on knowing the weight of the aircraft. However, the precise passenger payload weight is unknown and pilots rely on estimates that are often out of date and may not reflect the current population demography.
Methods: This paper explores the effects an increasing passenger weight payload has on key performance characteristics of commercial aircraft. A passenger demographic model is developed based on varying body mass index levels. Aircraft performance characteristics are determined from established analytical methods to examine three aircraft types. Comparisons are made between standard passenger weights from key aviation regulators around the world with scenarios reflecting various degrees of obesity prevalence. These scenarios are further compared to global variation across different regions around the world.
Findings: In parts of Africa and Asia that have low obesity prevalence but use standard passenger weights are overestimating aircraft performance characteristics, particularly fuel costs. Juxtaposed, regions of higher obesity prevalence such as those encompassing westernised nations may begin to see significantly compromised safety margins if increasing weight trends continue.
Conclusions: Overall performance characteristics for any aircraft type considered in this study will be significantly affected should existing obesity growth forecasts for the next decades are proven to be accurate. Thereby, justifying the need for more accurate regulations and improved flight operational procedures.

1. Introduction

It is widely known that the average person's weight is increasing and obesity has become a global problem especially in developed regions (NCD Risk Factor Collaboration, 2016c; Wang and Lim, 2014; Finucane et al., 2011). The World Health Organisation noted that between 1975 and 2016 worldwide obesity prevalence tripled (WHO, 2016). Increasing body weight has many social implications, especially in health. People with a higher body mass potentially become more susceptible to diseases such as diabetes, vascular disorders or muscular-skeletal problems. Management and preventing direct health effects can be costly to society. Further, there are other secondary and tertiary indirect costs to the economy due to obesity (Ananthapavan et al., 2014; Hammond and Levine, 2010); for example, Lobstein (2015) highlights that medical costs relating to associated obesity health issues cost $150 billion to the economy of the United States of America and £5 billion for the United Kingdom.

Pertinent issues encompassing changes in airline passenger anthropometry focus primarily on passenger comfort and experience (Vink and van Mastrigt, 2011; Ahmadpour et al., 2014; Patel & D'Cruz, 2017). Passengers of all sizes feel discomfort during flight, especially long-haul flights. Aircraft seat pitches (distance between two rows) have generally decreased in size with most airlines offering a seat pitch between 30 and 32 inches (Vasel, 2017). However, larger framed passengers experience greater discomfort

* Corresponding author.
E-mail address: s3198416@student.rmit.edu.au (D.J. Melis).

https://doi.org/10.1016/j.jth.2019.03.003
Received 5 January 2019; Received in revised form 4 March 2019; Accepted 5 March 2019
Available online 22 March 2019

owing to the tight spaces available; this then places a stigma on these passengers by both cabin crew and fellow passengers (Small and Harris, 2012; Mylrea, 2009; Bolton, 2004).

Commercial aviation continues to grow with largely falling airfares and increasing demand, particularly in emerging economies. Airlines continue to balance customer expectations for high levels of service while striving to maintain profitability and market share. This situation is further complicated by the demand for continual safety improvements and efficiency increases. These drivers have led to substantial research into technologies that predominantly strive to make aircraft operations more efficient: bio-fuels, light-weight materials, more aerodynamic designs and advancements in air traffic management. Despite the advances across all these areas, Melis et al. (2018) have demonstrated that there is a limited amount of research being conducted exploring the issues associated with anthropometrical changes of commercial aviation passengers, which is a key factor impacting the performance of commercial aircraft.

A significant cost for airlines is the fuel expenditure. Global fuel demand is expected to rise 1.9% annually between 2008 and 2025 (Chèze et al., 2011). Conjunctly, as fuel usage increases so too the greenhouse emissions produced by aircraft. The International Civil Aviation Organisation (ICAO) has estimated that for every kilogram of aviation fuel burnt, 3.157 kg of carbon-dioxide emissions is produced (International Civil Aviation Organisation, 2014). Surprisingly, the effects of the relationship between aircraft fuel burnt and passenger weight are limited to a few studies only.

Dannenberg et al. (2004) initially estimated 1.3 billion litres of extra fuel due to excess weight in the decade around 1994 in the USA. A comprehensive study by Tom et al. (2014) of the USA domestic transport systems for 1970–2010 has been conducted, showing that 95.2 billion litres of extra fuel was required by the domestic aviation sector due to excess passenger weight. This resulted in a net output of 238 billion metric tonnes of additional greenhouse emissions, from $37 billion USD (adjusted to 2012) of extra fuel. In another geographical context, a recent study by Melis et al. (2017) estimated the Australian domestic commercial aviation sector had used 561 kilo-tonnes of fuel between 1990 and 2014 to transport 15.8 tonnes of excess passenger weight at the cost of A$411.7 million dollars. Further, 1.7 million-tonnes of equivalent carbon-dioxide were released into the atmosphere. Yin et al. (2015) has explored the greenhouse emissions produced by international flights for selected Australian routes using actual passenger and cargo data from airlines. Their study compared aircraft and airline frequency to determine greenhouse emissions rely not only on aircraft type and passengers but also on cargo payload.

Various studies have explored the fuel saving measure for the different phases of a flight. Fuel savings during the ground phase can vary greatly from various airport layouts through improved ground operating procedures (Khadilkar and Balakrishnan, 2012); for example taxi scenarios consisting of multiple stops and starts can experience 18% higher fuel requirements (Nikoleris et al., 2011). Aircraft can be held on the ground for a considerable time and often the pilot may request a single engine taxi to potentially save fuel. Fuel savings are also explored during the climb and descent phases (Soler et al., 2012; Slater, 2002). However, these savings are explored from an operational point of view. Ultimately, the cruise portion of the flight consumes the majority of the fuel depending on the range. Dalmau and Prats (2015) highlight that for a continuous cruise climb profile phase; fuel savings range from 0.5% to 2% for a narrow body aircraft, whilst for a wider body aircraft potential savings sit between 1% and 2%. In the same way, Turgut et al. (2014) demonstrate that a reduction of one tonne of aircraft mass can result in 15–21 kg less of hourly fuel consumption, based on statistical data.

Kaivanto and Zhang (2018) developed a new metric for idealised optimal flight segmentation based on the Breguet range equations and the weight model presented by Küchemann (1978). Their approach verifies the conventional representation of the payload-fuel-efficiency metric and complements the model with new findings. The payload-fuel-efficiency metric proposed by these authors gives direction on comparing the efficiency levels of multiple aircraft with different design ranges, including aircraft that can be grouped to serve a flight route containing multiple segments. Similarly, Hileman et al. (2008) incorporate the specific energy of aviation fuel into the payload–range efficiency metric to highlight the energy costs for a given range and payload. They highlight that due to the advent of new technologies there has been a 51% increase in payload-fuel-energy efficiency between 1991 and 2007.

Understanding the demographic composition of the passenger payload can play an important role in understanding the performance characteristics of an aircraft. For example, some airlines operate fly-in-fly-out (FIFO) operations. In this context, FIFO operations consist of primarily charter flight operations that transport workers to remote locations; such as mines and off-shore oil platforms. Generally, FIFO workers are predominantly male and characterised as being more overweight than the general public and other industry sectors (Barclay et al., 2013). In a study by Joyce et al. (2013), 79.3% of the FIFO workers surveyed were either overweight or obese. This proportion is higher than the average of 56% in the National Health and Nutrition Examination Survey (NHANES) 2013–2014 data (CDC, 2015). Aircraft operated on FIFO missions are generally narrow-bodied 90 to 150 seat aircraft, such as Boeing 717, Embraer 170/190 and Fokker 100. In an emergency, these aircraft carry large FIFO workers who may have added difficulty in exiting the aircraft through the emergency overwing exits as these are often smaller than those on larger narrow-bodied aircraft.

Similar to FIFO operations, airlines providing contracts for transporting military personnel have to consider the difference in additional carry-on weight of individual military equipment. In most cases, this additional carry-on weight may not match the civilian standards being used by the charter airline. One such instance was that of Arrow Air in 1988 in Gander, Canada. Part of the cause of the fatal crash was that the pilots estimated the military personnel weight using standard passenger weight issued for civilian flight. The consequence was that the pilots underestimated the weight and thus failed to calculate the incorrect thrust required for take-off and take-off distance (CASB, 1988).

The opposite can be true; pilots may overestimate the passenger payload causing incorrect trim conditions resulting in increased fuel burn due to drag from incorrect attitude settings. One such occurrence occurred to a Qantas flight that was carrying a large number of school children. In this event, the pilots were not aware that the children were on-board and subsequently calculated the passenger weight to be comprised of adults. It was only at the lift-off that the pilots noticed that the aircraft was nose heavy; as the children were seated at the rear of the cabin. As a consequence, the pilots exceed the calculated lift-off speed calculated by 25 knots and potentially used more runway distance (ATSB, 2014).

A study by Van Es (2007) surveyed occurrences relating to weight and balance issues of aircraft and noted from the collated data, 1.9% of passenger flights had incorrect payload information. A notable incident was that of Midwest Airlines Flight 5481 in 2003, the aircraft experienced a tail heavy attitude during take-off and subsequently stalled and crashed due to improper weight and balance. The investigation noted, in part, that a contributing factor was that inaccurate weight estimation of the passengers (NTSB, 2004). As part of the recommendations, the National Transport Safety Board recommended that the passenger weight standards should be updated. In fact, weight and balance is a key factor in determining the stability and performance of the aircraft. By knowing the centre of gravity position relative to the mean aerodynamic centre, the pilot can elevate the moment created by setting the correct trim condition. It has been noted that pilots rely heavily on the standard passenger weight estimators for weight and balance and that an in-flight centre of gravity position estimator could be used to improve cruise flight trim and fuel savings (Chaves et al., 2018).

The literature has not explored the detailed effects of aircraft flight and ground performance characteristics concerning passenger weight changes. Aircraft experience different conditions for each consecutive flight, particularly for characteristic change depending on the weight of the aircraft. Manufacturers provide airlines with detailed performance charts and data in aircraft manuals, technical documents and on-board software packages to calculate flight performance. These software packages calculate everything from arrival to departure; ground characteristics such as take-off distance, lift-off and landing speeds and distances; flight characteristics such as climb thrust, cruising speed and distances and particularly fuel consumed, are all calculated with the on-board computer.

Although aircraft experience different passenger payloads for consecutive missions the long-term implication of increasing passenger weight changes have not been analysed. This paper uses established analytical methods to explore the effects of passenger weight change on selected aircraft mission performance attributes. Three types of aircraft will be explored; narrow-body (turbofan) Airbus A320, wide-body (turbofan) Airbus A330-200 and regional commuter (turboprop) aircraft Avions de Transport Regional ATR-72. The paper aims to answer two situations related to passenger weight and obesity. Firstly, how the current obesity environment impacts the selected flight parameters about current standard weights recommended by leading national aviation regulatory authorities; secondly how different scenarios of varying obesity prevalence will affect the same selected flight parameters.

2. Analytical method

2.1. Data sources

The model presented in this paper is based on data collected from various sources, such as aircraft handling documents for aircraft weights; the International Civil Aviation Organisation (2017) engine emissions databank for engine information (e.g. maximum thrust and fuel flow at particular phases of flight at certain thrust levels); and reference literature on aircraft performance, including Sadraey (2017), Filippone (2012), Niţă (2008), Howe (2000), Eshelby (2000) and McCormick (1995).

Furthermore, the aforementioned reference texts provide examples and case studies of particular aspects of flight that can be compared to verify the analysis developed in this paper. Additionally, literature cited in Section 1 contributes with some examples for comparison purposes. A flight plan for an A320 flight between Singapore and Male (SIN-MLE) was obtained from an undisclosed airline source. This flight flew 3,060 km and used 11.6 tonnes of fuel and carried 13.9 tonnes of payload. Additional comparisons are made using the Airbus issued Aircraft Characteristics - Airport And Maintenance Planning document for the A320 and A330 aircraft (Airbus 2014, 2015).

The characteristics of the population weight and obesity profiles were obtained from the National Health and Nutrition Examination Survey 2013–2014 report issued by the Centre for Disease Control in the United States of America (CDC, 2015). Additional global data is sourced from the Global Health Observatory Data from the World Health Organisation (WHO, 2016) and the NCD Risk Factor Collaboration (2016a), in which the individual country data in the later is divided into several categories based on regions (Table 1).

2.2. Passenger characteristics

Two passenger models are presented; the first describes the current situation for various nations around the world, the second incorporates changes in the overall obesity prevalence using a sample population from NCD Risk Factor Collaboration (2016a) with constant BMI category ratios.

Table 1
Obesity prevalence of nine regions around the world, as stipulated by NCD Risk Factor Collaboration (2016a).

Region Name	Region Number	Obesity Prevalence (mean% ± SD)
Sub-Saharan Africa	1	28.21 ± 8.4
Central Asia, Middle East and North Africa	2	57.63 ± 11.6
South Asia	3	24.62 ± 3.5
East and South East Asia	4	57.82 ± 12.1
Oceania	5	71.81 ± 10.1
High Income Asia Pacific	6	61.31 ± 5.6
Latin America and Caribbean	7	57.00 ± 5.7
High Income Western Countries	8	59.67 ± 3.6
Central and Eastern Europe	9	53.92 ± 9.3

Table 2
BMI categories with associated BMI range values, as issued by the World Health Organisation (2016).

BMI Category	BMI Range (kgm^{-2})	i
Under	Less than 18.5	1
Normal 1	18.5 to 19.9	2
Normal 2	20.0 to 24.9	3
Overweight	25.0 to 29.9	4
Obese 1	30.0 to 34.9	5
Obese 2	35.0 to 39.9	6
Morbid Obesity	Greater than 40	7

i is used in successive equations

2.2.1. Modelling current situation

NCD Risk Factor Collaboration (2016a) obesity data is provided for 200 countries around the world from 1975 until 2014. The data presents the level of obesity along with the WHO BMI categories as shown in Table 2 Additional information is provided by NCD Risk Factor Collaboration (2016b) data providing the mean height of males and females. Data from this source does not account for age groupings.

Using only the prevalence percentages of each BMI category, known heights and population percentages for each gender, an average weight for each BMI category are calculated from Eq. (1). Where $\overline{BMI}_i$ is the average BMI value for a given category i, and $h_{(G)}$ is the average height for a given gender.

$$\bar{W}_{i(G)} = \overline{BMI}_i h^2_{(G)} \tag{1}$$

Eq. (2) determines the proportion of the population that fits within a particular BMI category, where $P_{(G)}$ is the percentage of the population for a given gender and $P_{(i\cup G)}$ is the proportion of the BMI category within the given gender. The weight of the passenger payload is then determined by resorting to Eq. (7).

$$P_{i(G)} = P_{(G)} P_{(i\cup G)} \tag{2}$$

2.2.2. Modelling for different scenarios

Anthropometric data has been sourced from the Centre for Disease Control and Prevention biennially survey known as NHANES (National Health And Nutrition Examination Survey). This survey covers the populations of the USA and provides a large sample of current physical characteristics, such as height, weight, BMI and age. This information was sorted into age and BMI categories for the sake of a more practical approach. The NHANES data contained $n = 5229$ sample individuals with useable data of which 47.5% and 53.5% are male to female respectively.

Once the data was sorted into their respective categories, the next step consisted in determining the proportion of the given population size (n) with a specific BMI category i (Table 2). For an age group and gender (A,G), the number of the elements of that set is divided by the total number of elements in the population as shown by Eq. (3). These values are shown in Table 3a and b

$$P_{i(A,G)} = \frac{n_{i(A,G)}}{\sum n_{(A,G)}} \tag{3}$$

Eq. (4) describes the sum of the element weights for a given BMI category (i) for an age group and gender (A,G). It is then divided by the number of elements in that group to determine the average weight for that particular age group and gender (A,G). The results are shown in Table 4a and b.

$$\bar{W}_{i(A,G)} = \frac{\sum W_{i(A,G)}}{n_{i(A,G)}} \tag{4}$$

Table 3a
Percentage of the male population by age and BMI category from the NHANES data.

BMI	Under	Normal 1	Normal 2	Over	Obese 1	Obese 2	Morbid	Total
Age								
18–24	0.98%	0.40%	2.10%	1.42%	1.03%	0.46%	0.23%	6.6%
25–34	1.13%	0.38%	2.14%	2.12%	1.26%	0.34%	0.48%	7.9%
35–44	1.11%	0.36%	1.64%	2.20%	1.45%	0.61%	0.25%	7.6%
45–54	1.13%	0.33%	1.80%	2.22%	1.22%	0.42%	0.42%	7.5%
55–64	1.19%	0.40%	1.80%	2.24%	1.30%	0.55%	0.46%	7.9%
65–74	0.63%	0.27%	1.30%	1.63%	0.96%	0.55%	0.29%	5.6%
75+	0.63%	0.15%	1.07%	1.15%	0.90%	0.17%	0.23%	4.3%
Total	6.79%	2.29%	11.86%	12.97%	8.13%	3.12%	2.35%	47.50%

Table 3b
Percentage of the female population by age and BMI category from the NHANES data.

BMI	Under	Normal 1	Normal 2	Over	Obese 1	Obese 2	Morbid	Total
Age								
18–24	1.19%	0.48%	1.76%	1.91%	1.05%	0.44%	0.42%	7.2%
25–34	1.07%	0.40%	2.07%	2.05%	1.15%	0.73%	0.55%	8.0%
35–44	1.51%	0.42%	2.45%	2.12%	1.53%	0.90%	0.27%	9.2%
45–54	1.40%	0.33%	1.78%	1.97%	1.45%	0.75%	0.63%	8.3%
55–64	1.28%	0.57%	1.84%	2.26%	1.26%	0.63%	0.65%	8.5%
65–74	1.15%	0.23%	1.47%	1.76%	1.09%	0.52%	0.48%	6.7%
75+	0.96%	0.23%	1.17%	1.13%	0.55%	0.36%	0.15%	4.6%
Total	8.55%	2.66%	12.53%	13.20%	8.09%	4.32%	3.16%	52.50%

Table 4a
Average weight of men calculated from NHANES data and categorised by age and BMI category.

BMI	Under	Normal 1	Normal 2	Over	Obese 1	Obese 2	Morbid
Age							
18–24	29.4	51.1	63.6	78.0	90.9	109.1	128.7
25–34	26.9	49.1	64.1	80.6	93.0	104.4	130.5
35–44	24.6	45.3	62.7	80.1	93.1	107.7	123.2
45–54	27.9	43.7	63.0	82.1	93.7	108.9	129.8
55–64	26.6	40.0	61.6	78.7	94.2	105.4	132.7
65–74	28.0	46.1	63.1	76.5	93.3	102.4	127.7
75+	25.9	48.9	61.8	77.4	93.8	103.0	127.4

Exploring the effects of passenger weight changes for this paper is dependent on the prevalence of obesity being modelled. The total percentage of $(P^{j}_{BMI>25})_{(G)}$ is determined by Eq. (5), where *REF* is the reference value calculated from NHANES and *j* represents the obesity prevalence in percentage. The same equation is used to evaluate the percentage of BMI < 25.

$$(P^{j}_{BMI>25})_{(G)} = (P^{REF}_{BMI>25})_{(G)}\left(\frac{P^{j}_{BMI>25}}{P^{REF}_{BMI>25}}\right)_{Total} \tag{5}$$

Using the same process as Eq. (5), the proportion of a newly estimated sample size *j* was determined with Eq. (6). Where *REF* denotes the reference value calculated from NHANES. This value is then used in the following section in Eq. (7) (section 2.3.1) to calculate the passenger payload weight.

$$P^{j}_{i(A,G)} = (P^{j}_{BMI>25})_{(G)}\left(\frac{P_{i(A,G)}}{(P_{BMI>25})_{(G)}}\right)_{REF} \tag{6}$$

2.3. Passenger payload and fuel fraction relation

2.3.1. Passenger payload

It is assumed that the model explores the effect of obesity of an adult population; therefore aircraft are assumed to carry no passengers under the age of 18 years. The second assumption is that the demographic distribution of adults of the NHANES population mirrors the aircraft passenger payload population. The final assumption is that the aircraft has a 100% load factor. However, airline statistics show that load factors on domestic markets can range from 75% to 85% (Arul, 2014; Mazarrati et al., 2009).

The total weight of the passenger payload (W_{pax}) is limited by the capacity of that aircraft. Knowing the proportion of the particular BMI group and the average weight of that group, the total weight for that BMI group on board the aircraft can be determined using Eq. (7), where *N* is the aircraft passenger capacity. It is important to note that the value of $NP_{i(A,G)}$ will be an integer, as there cannot be a fraction person on an aircraft. If the value is rounded to the nearest smaller whole number, the value representing the number of passengers is underestimated, for lower capacity aircraft and towards the outer extremes of the BMI range.

$$W_{pax_{i(A,G)}} = NP_{i(A,G)}\bar{W}_{i(A,G)} \tag{7}$$

Once the weight for the individual category is calculated, the total sum of the passenger payload can be determined by using Eq. (8).

$$W_{pax} = W_{(BMI>25)} + W_{(BMI<25)} \tag{8}$$

where,

$$W_{(BMI>25)} = \sum_{i=4,5,6,7} W_{pax_{i(A,G)}} \qquad W_{(BMI<25)} = \sum_{i=1,2,3} W_{pax_{i(A,G)}}$$

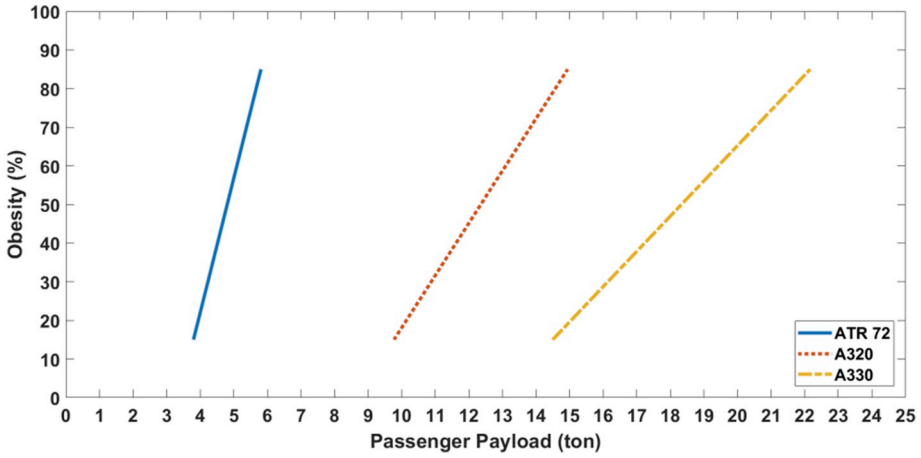

Fig. 1. Aircraft passenger payload for the three aircraft at various obesity levels.

This study explored one set of conditions relating to BMI demographics. In each case the underlining ratio between the higher BMI categories remained constant, i.e. the ratio of Under, Normal 1, Normal 2, Over, Obese 1, Obese 2 and Morbid remains the same. The model is capable of determining the payload (passenger) weight based on any given aircraft capacity and total obesity prevalence. Conducting the study in this manner, therefore, does not take into account the various BMI categories periodic change, as the scope of this paper is to compare current obesity prevalence trends implications while using current passenger weight standards.

Additional passenger payload scenarios using standard weights based on the ICAO, Federal Aviation Administration (FAA), Europe, European Aviation Safety Authority (EASA) or Civil Aviation Authority UK (CAA UK) are used to establish a baseline comparison. ICAO uses a standard 80 kg per passenger regardless of passenger gender or ratio. FAA uses a 60:40 male to female ratio at 83 kg and 73 kg respectively. EASA established weights of 95 kg and 75 kg for male and female respectively, while CAA UK have male and female weights of 88 kg and 70 kg respectively. An additional estimation of passenger baggage (W_{BAG}) is added to the overall payload, assuming that each item of luggage is 25 kg and that 70% of the passengers take one bag and 30% take two bags. The model assumes that no additional air freight or cargo is carried for simplicity purposes. The payload weight is added to the operational empty weight (OEW) of the aircraft to determine the zero-fuel weight (ZFW) (Eq. (9)). In an optimal situation, at the end of a flight, an aircraft would ultimately have the exact fuel to have only the reserve fuel plus payload and the operational empty weight. Fig. 1 shows the passenger payloads calculated for each aircraft at the different obesity prevalence levels.

$$ZFW = OEW + W_p + W_{BAG} \tag{9}$$

2.3.2. Fuel fraction, cost and emissions

An aircraft's range performance is often determined by the non-dimensional factor known as the fuel fraction or zeta value (ξ). Knowing that the fuel fraction must be the same as the change in weight, ξ can be determined from Eq. (10). The fuel fraction value thus can be used to illustrate the effects of payload weight variation on the range of an aircraft.

$$\frac{W_j}{W_i} = 1 - \frac{\Delta W}{W_i} = 1 - \xi \tag{10}$$

Substituting the assumed final weight of the aircraft as the zero-fuel weight (ZFW) from Eq. (9) into Eq. (10), the initial aircraft weight can be determined from Eq. (11).

$$W_i = \frac{ZFW}{1 - \xi} \tag{11}$$

The fuel used by the aircraft (W_f) can be calculated either from fuel flow (Q), time (t) and or directly from the fuel fraction (Eq. (12)).

$$W_f = Q_i t = W_i \xi \tag{12}$$

The fuel price is updated regularly and can be found on numerous online sources; an October 2018 listed fuel price of $751.12 USD per metric tonnes was used in this paper (IATA, 2018). Fuel cost is calculated using Eq. (13), where i represents a different flight phase. Similarly, the pollutants can be calculated using Eq. (14) using the emissions index (EI_i) listed in the ICAO engine emissions databank presented as a unit of a pollutant for a unit of fuel burnt, where i represents the different pollutants.

The ICAO databank provides engine performance and emissions data acquired from full-scale engine tests at sea level for the idle, climb, descent and take-off segments of flight. For the vast majority of jet and turbofan commercial engines, it provides values of fuel flow (kgs^{-1}) and emission indices (grams of pollutant emitted per kilograms of fuel burnt) taken at 7%, 30%, 85% and 100% rated thrust outputs. The pollutants included in the databank are hydrocarbons, carbon monoxide, and nitric oxides. Furthermore, it was

Table 4b
Average weight of women calculated from NHANES data and categorised by age and BMI category.

BMI	Under	Normal 1	Normal 2	Over	Obese 1	Obese 2	Morbid
Age							
18–24	29.06	46.46	59.96	76.59	89.67	101.53	122.56
25–34	28.83	48.24	60.28	75.77	86.79	99.64	126.11
35–44	27.04	44.90	60.88	72.54	89.02	97.86	127.86
45–54	27.53	45.11	60.98	74.64	88.24	99.15	121.31
55–64	26.89	47.40	59.46	75.05	86.78	101.66	121.61
65–74	25.91	49.07	60.83	73.75	85.96	93.91	124.32
75+	24.54	53.03	60.29	73.36	85.47	98.70	136.45

considered that 3.157 kg of carbon-dioxide is emitted for each kg of aviation fuel burnt to estimate the total emissions associated with the cruise flight segment (International Civil Aviation Organisation, 2014).

$$Fuel\ Cost = \sum_i W_{fi} f_{price} \tag{13}$$

$$Emissions = \sum_i W_f EI_i \tag{14}$$

2.4. Aircraft characteristics

Three types of aircraft are examined in this paper: narrow-body Airbus A320, wide-body Airbus A330-200 (A330-200) and turboprop aircraft Avions de Transport Regional ATR-72. The aircraft characteristics are shown in Table 5. These aircraft are frequently utilised aircraft platforms in service by many airlines around the world. The model presented herein explores the flight characteristics from a single take-off to landing cycle, excluding loiter and taxi. Key assumptions include, no additional cargo is carried, headwinds and tailwinds, additional fuel for holding patterns and alternative airports are all not considered, similarly regulatory mandated fuel reserves, and the International Standard Atmospheric conditions are observed. Calculated characteristics in Table 5 are derived from methods outlined by Howe (2000), such as TSFC and lift to drag ratio, which are then compared to values given by Babikian et al. (2002) and Roskam (1985).

Table 5
Key aerodynamic and propulsive characteristics of the three aircraft types considered in this study.

Characteristic	Narrow-body	Wide-body	Turboprop
Aircraft	A320[a]	A330-200[b]	ATR 75[c]
Capacity	180	267	70
Maximum Take-off Weight (MTOW) (tonnes)	73.5	238	23
OEW (tonnes)	41.3	120.2	13.5
Wing Area (S) (m^b)	124.0	361.6	61.0
Aspect Ratio	10.34	10.06	12.00
Zero-Lift Drag Coefficient (C_{Do})[f]	0.01296	0.0123	0.0274[g]
Induced Drag Coefficient (k)[f]	0.0422	0.0447	0.0342[g]
Cruise Mach Speed (M)	0.79	0.82	0.42
Engine Model	CFM56-5b	Trent 700	P&W PW127[e]
Maximum Thrust per engine (T_0)[d] (kN)	117.9	299.1	
Shaft Horse Power per engine (P)[e] (HP)			2132
Bypass Ratio (β)[d]	5.9	5.07	
Propeller Efficiency (η)[g]			0.859
Thrust Specific Fuel Consumption[f] (c_{TF}) ($NN^{-1}s^{-1}$)	15.9×10^{-5}	16.2×10^{-5}	
Power Specific Fuel Consumption[e] (c_{TP}) ($NW^{-1}s^{-1}$)			85.0×10^{-7}
Idle Fuel Flow (kg s^{-1}) [d] per engine	0.107	0.243	0.051[e]
Take-off Fuel Flow (kg s^{-1})[d] per engine	1.166	2.886	0.165[e]
Climb Fuel Flow (kg s^{-1}) [d] per engine	0.961	2.353	0.139[e]
Descent Fuel Flow (kg s^{-1}) [d] per engine	0.326	0.783	0.085[e]

[a] (Airbus, 2015).
[b] (Airbus, 2014).
[c] (ATR DC/E 2014).
[d] (International Civil Aviation Organisation, 2017).
[e] (Avions de Transport Regional, 2001).
[f] Calculated values using methods from Howe (2000).
[g] (Niță, 2008).

2.5. Aircraft performance calculations

A performance model was built to investigate the effects of passenger weight change on mission performance. A detailed model and corresponding aircraft performance calculation steps are presented in the appendix section of this paper. The effects of passenger weight change were calculated for key flight phases, namely cruise range, climb and descent and take-off and landing.

2.5.1. Aircraft range during cruise

There are three types of cruise regimes, namely; constant lift coefficient and velocity; constant lift coefficient and altitude; constant velocity and altitude. For this paper, only the cruise regime of constant velocity and constant altitude will be explored. The model developed in this paper aims to explore the changes in flight conditions where the only variable is aircraft payload variations due to obesity. Thus, certain parameters, particularly Mach speed and altitude, are kept constant. Therefore, integrating the Breguet range equation (see appendix A) yields Eq. (15) for a turbofan aircraft whereas Eq. (16) is used for a turboprop aircraft.

$$X_{\mathrm{TF}} = \left[\left(\frac{2VE_{max}}{c_{TF}}\right)\right]\tan^{-1}\left(\frac{E\xi}{2E_{max}(1 - kC_L E\xi)}\right) \tag{15}$$

$$X_{\mathrm{TP}} = \left[\left(\frac{2\eta E_{max}}{c_{TP}}\right)\right]\left[\tan^{-1}\left(\frac{2\frac{ZFW}{(1-\xi)}}{\rho V^2 S\sqrt{C_{Do}/k}}\right) - \tan^{-1}\left(\frac{2ZFW}{\rho V^2 S\sqrt{C_{Do}/k}}\right)\right] \tag{16}$$

Where V is velocity, E is lift to drag ratio, $E_{\max}$ is maximum lift to drag coefficient, c_{TF} is thrust specific fuel consumption (TSFC) and c_{TP} is power specific fuel consumption (PSFC), ξ is fuel fraction, k is induced drag factor, ZFW is the zero-fuel weight and η is propeller efficiency.

2.5.2. Climb and descent

The rate of climb (ROC) characteristics is established by determining the take-off weight from a calculated fuel fraction value for a cruise situation. The calculated velocity is for the climb phase (see Appendix B) with its associated Mach number for a given altitude is used to determine the thrust (see Appendix A). Finally, the ROC for the turbofan and turboprop are determined using Eq. (17a) and Eq. (17b) respectively. The rate of descent (ROD) is present when ROC has negative values (see Appendix B).

$$ROC_{TF} = \frac{(TV - DV)}{W} \tag{17a}$$

$$ROC_{TP} = \frac{(P\eta - DV)}{W} \tag{17b}$$

Then the total fuel used is determined by multiplying the fuel flow by the time to climb considering the fuel flow data for a particular engine type issued in the ICAO database. The time to climb (t_{clb}) is determined by Eq. (19). Where h is the desired altitude, j is either climb or descent and i represents the ROC or ROD at an increment of altitude.

$$t_j = \sum_{i=0}^{n}\left(\frac{\Delta h}{ROj_i}\right) \tag{19}$$

2.5.3. Take-off and landing

Take-off and landing consist of three parts, an airborne phase; a rotation phase and a ground phase. Key velocities are based on the stall speed (V_s), Eq. (20). V_1 or $V_R = 1.1V_s$, V_{LO} & $V_{TD} = 1.2V_s$, $V_2 = 1.3V_s$; these values were taken from Sadraey (2017), and similar approximations are also expressed in Filippone (2012) and Eshelby (2000). They are based on FAR regulation Part 25 which also specifies that a transport aircraft must clear a 50 ft obstacle for the take-off and landing manoeuvres.

$$V_s = \sqrt{\frac{2W}{\rho S C_{lmax}}} \tag{20}$$

A take-off/landing field distance (D_Z), where, Z is take-off or landing, is calculated in Eq. (21). It is the sum of the distance travelled during the three phases; the ground roll (X_{grd}), rotation (X_{rot}) and the airborne phase until the clearance height (X_{air}) (see Appendix D).

$$D_z = (X_{grd} + X_{rot} + X_{air})_z \tag{21}$$

The time spent during each take-off phase is calculated from Eq. (22), where ΔX_z is the change in distance, ΔV_z is the change in speed and Z is the ground, rotation or airborne phase. Then using the fuel flow data for a particular engine type, the total fuel used is determined.

$$t = \sum_{z}\frac{2\Delta X_z}{\Delta V_z} \tag{22}$$

Table 6
Calculated performance characteristics for three aircraft with specified flight parameters based on standard passenger weights from key aviation regulatory bodies.

	Fuel Used (kg)	Fuel Cost (USD)	Emissions Produced (ton)	Time to Climb (min)	Fuel to Climb (kg)	Take-off Distance (m)	Landing Distance (m)
A320 - Range 3,000 km, Cruise altitude 36,000 ft, M = 0.79							
ICAO	9213.7	6955.3	19.42	18.02	2077.6	1744.1	1352.7
FAA	9167.7	6920.5	19.32	17.81	2053.5	1734.4	1341.9
EASA	9453.0	7135.9	19.82	18.91	2181.2	1980.9	1397.8
CAA UK	9191.5	6938.5	19.37	17.91	2065.5	1884.2	1347.3
A330-200 - Range 7,500 km, Cruise altitude 36,000 ft, M = 0.82							
ICAO	46,704.7	30,873.7	129.24	15.05	4249.4	1850.7	1338.2
FAA	46,647.1	30,830.6	129.06	15.01	4236.7	1856.7	1334.8
EASA	47,187.0	31,234.7	130.75	15.43	4356.6	1906.4	1366.3
CAA UK	46,647.1	30,830.6	129.06	15.01	4236.7	1850.7	1334.8
ATR 72 - Range 700 km, Cruise altitude 25,000 ft, M = 0.42							
ICAO	1441.1	1087.9	2.88	23.62	2724.3	1408.7	997.9
FAA	1434.2	1082.6	2.86	23.16	2671.0	1384.8	1008.6
EASA	1471.9	1111.1	2.94	25.70	2963.5	1689.0	1052.7
CAA UK	1437.6	1085.2	2.87	23.39	2697.5	1396.7	1003.3

3. Results and discussion

The specific results discussed in section 3 focuses on a simplified particular mission for each type of aircraft: 1) the narrow-body aircraft mission profile consists of a range of 3000 km flying at a cruise Mach of 0.79 at an altitude of 36,000 ft (FL360); 2) the wide-body aircraft mission profile with a range of 7500 km flying at a cruise Mach of 0.82 at an altitude of 36,000 ft; and 3) the turboprop aircraft mission profile consisting of a range of 900 km flying at a cruise Mach of 0.42 at an altitude of 25,000 ft (FL250). Table 6 provides results corresponding to the three aircraft for the performance factors using the passengers' weights defined by ICAO for purposes of comparison to standardised weights issued by regulators; the USA, FAA; Europe, EASA and the UK, CAA UK. In the absence of self-developed standards, many nations may opt to follow either of these regulators. Out of the four regulators, EASA have

Table 7
Difference between standard weights and average weight for selected countries with different obesity prevalence.

Country	BMI > 25 (%)[a b]	Average weight (kg)		Standard weight (kg)		
		Male[a b]	Female[a b]	Male	Female	Regulator[c]
Antigua and Barbuda	59.5	77.6	***72.6***	74	64	ECCAA
Australia	63.6	***84.1***	***70.1***	81.8	66.7	CASA
The Bahamas	63.9	***77.9***	***71.9***	74	64	BCAA
Canada	64.5	***83.7***	69.5	83	73	TC
Costa Rica	59.9	72.8	62.7	88	70	DGAC
Europe[d]	56.3	80.6	66.1	94	75	EASA
El Salvador	56.1	72.7	62.8	88	70	AAC
Fiji	63.3	***77.7***	72.8	77	77	CAAF
Ghana	32.2	65.1	61.9	83	73	GCAA
India	19.1	56.6	49.0	75	75	DGCA
Jordan	66.3	78.2	***72.1***	88	70	CARC
New Zealand	64.2	84.7	72.4	86	86	CAA NZ
Norway	58.8	84.6	68.4	88	70	CAA Norway
South Africa	52.2	69.8	***73.0***	88	70	SACAA
St Kitts and Nevis	57.9	***79.1***	***77.4***	74	64	ECCAA
St Lucia	54.3	***83.3***	***77.6***	74	64	ECCAA
Swaziland	39.9	67.1	***71.4***	88	70	SWACAA
Tanzania	23.7	60.9	57.3	88	70	TCAA
Trinidad and Tobago	57.9	79.9	***73.3***	88	70	TTCAA
Turkey	65.7	76.3	69.2	88	70	SHGM
UAE	70.1	76.6	70.0	88	70	GCAA
United Kingdom	63.1	82.6	69.7	88	70	CAA UK
USA	67.9	***89.3***	***75.5***	83	73	FAA

Italicised and **bold** text indicates that the standards are below the average weight.
Underlined highlights the standard weights used in this paper.
[a] (NCD Risk Factor Collaboration, 2016a).
[b] (NCD Risk Factor Collaboration, 2016b).
[c] Regulatory references are not included due to publication constraints.
[d] Average weight and obesity prevalence are determined by the average of all the individual European countries within the jurisdiction of EASA.

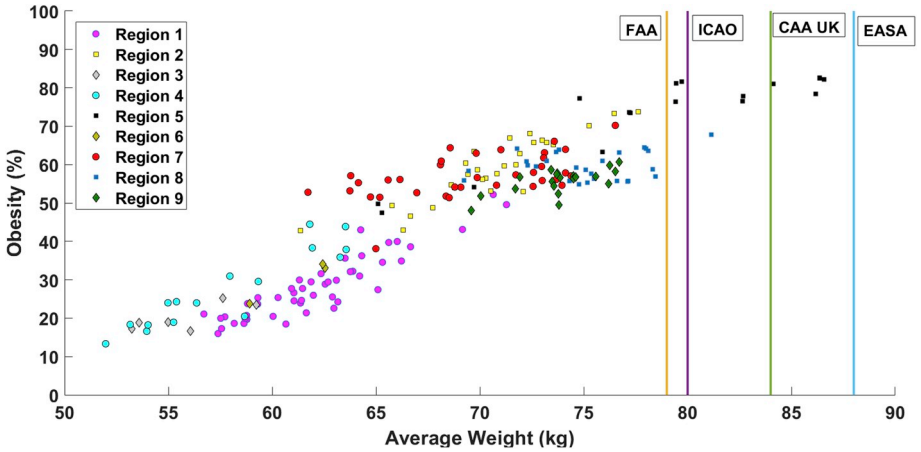

Fig. 2. Global weight averages for countries separated into regions by obesity prevalence with regulator standard weights.

updated their passenger weight standards as of 2009 (Berdowski et al., 2009). Consequently, the results of for an aircraft with the current passenger standards from EASA have higher results than those of the other regulators with lower standard weights.

3.1. Aircraft capacity and payload

Airlines thread a fine line between payload, range and fuel expenditure. Notwithstanding, pilots have to estimate the passengers' weight based on standard weights issued by the regulators which do not necessarily reflect operational circumstances accurately.

Furthermore, many nations around the world rely on either the regulations from the FAA, EASA or CAA UK. These nations generally lack the infrastructure or budget to carry out wide-scale passenger weight surveys as it happens in some other nations, such as Australia or Canada, which have adequate resources to perform regular surveys. Table 7 presents a comparison of the average weights and regulatory standards for selected countries along with their obesity prevalence. Among the selected countries, St Lucia has the highest difference between the average passenger weights and their standards with a difference in mass of 9.3 kg for males and 13.6 kg for females.

As previously mentioned, obesity is on the rise and consequently weight per passenger follows an identical increasing trend at a global scale. Currently the highest prevalence of BMI centres around the overweight and obese categories however, it is expected that this BMI prevalence will become more skewed towards the higher categories of obese and morbidly obese in the future. Gritsch et al. (2017) discuss that the Australian regulator standards became outdated within a decade of their inception. This study also suggested using the statistical health data on weight and obesity as a trigger to update the standards once the variance reaches 2%.

Regions 7, 8 and 9 (see Table 1) have less spread regarding obesity prevalence, and this can be attributed to the fact these regions encompass countries in Europe and the Americas. In these regions, there are diverse factors for different demographic ethnicities leading to a change in the overall dynamic of the demography of the people, thus on the average weight (Bil and Hanlon, 2016). As shown in Fig. 2 it can be seen that the average weight from many nations of the listed regions (Table 1) lie below the current weight standards from the key regulators.

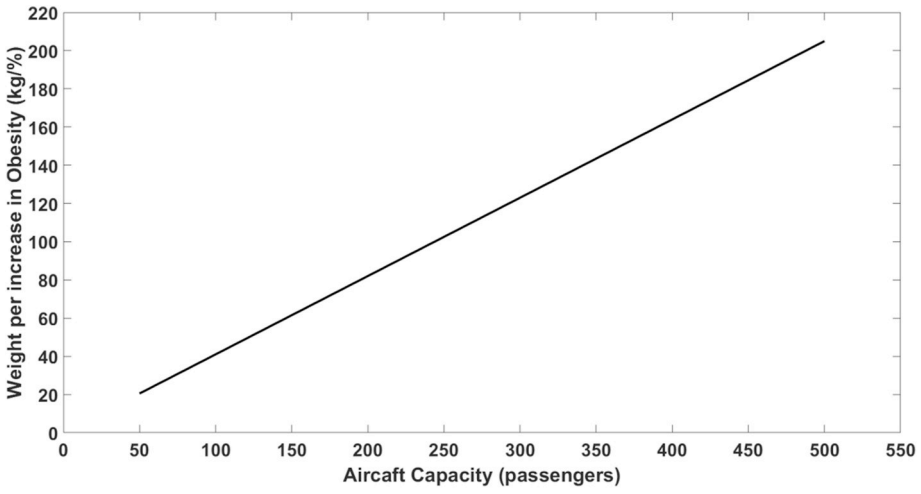

Fig. 3. Passenger payload weight per BMI increment for the number of seats in an aircraft.

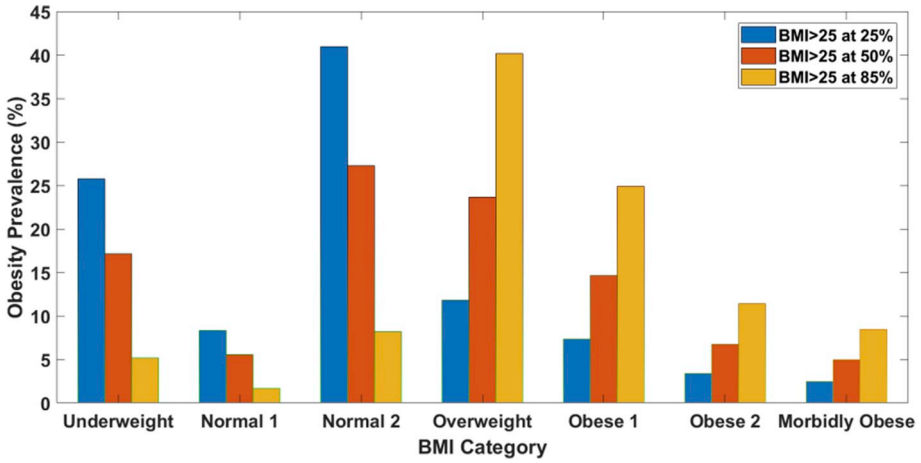

Fig. 4. Illustration of the constant ratios amongst the BMI categories change at different levels of overweight and obesity (BMI > 25) prevalence for use in this study. The data considered in this figure was sourced from the NHANES (CDC, 2015).

Taking into account the different BMI categories, Fig. 3 illustrates how the weight per change in obesity prevalence changes with aircraft capacity. The average weight of a passenger is based on the NCD Risk Factor Collaboration (2016a) data. By estimating the average weight in this manner we assume that the typical aircraft demography is a sample representation of the wider population. A key factor to note that has not been considered is the relationship between obesity and disposable income. The aviation industry's measure for capacity growth is the gross domestic product of a nation. The passenger model developed in this paper has not accounted for the effect of type of people travelling on a given flight. For instance, low-cost carriers attract financially savvy passengers due to lower airfares.

The data presented for NHANES represent the demographic situation of the USA for 2013–2014, with the consensus that the USA is a leading nation in the obesity problem. Other countries have distinct demographics depending on their social-economic contexts; some nations have lower relevancies of obesity, like in sub Saharan Africa [28.21% ± 8.4], whereas other nations such as those in the Oceania [71.81% ± 10.1] have higher relevancies at the more extreme BMI spectrum (NCD Risk Factor Collaboration, 2016c). Knowing this, the performance characteristics of specific aircraft types in those regions may vary greatly due to the difference in passenger payload. Fig. 3 illustrates how the amount of additional weight changes with a 1% increase in obesity for various aircraft capacities. It is evident that when aircraft capacity increases, more weight is added with a rise in obesity. Therefore, an aircraft with a capacity of 200 passengers will carry an extra 80 kg of extra passenger weight for every 1% rise in obesity prevalence.

3.2. Significances of increasing obesity prevalence

Each region is made up of nations with different demographics. Thomas et al. (2014) expect obese people in the USA (i.e. with BMI > 25) to plateau at 69% by 2030 while in the UK 71% by 2033. However, the proportions estimated for the obese category was greater than those for the overweight category. Currently, both have prevalence obesity of 67% and 63% respectively, with the overweight category dominating (NCD Risk Factor Collaboration, 2016c). An earlier study reported people with BMI > 30 to be 42% of the population by 2030 in the USA (Finkelstein et al., 2012).

The passenger characteristic model described in Section 2.2.2 is used to illustrate the effect of changing obesity scenarios. Fig. 4 shows the passenger BMI category prevalence used for the scenarios BMI > 25%, BMI > 50% and BMI > 85%. The scope of this paper looks at the overall obesity prevalence. The prevalence of the various obesity categories can change periodically. Thus the ratios between the BMI categories remained the same for the scenarios explored. The results obtained from these scenarios can then be extrapolated to the various regions around the world by adjusting the corresponding BMI ratios.

3.3. Range

Determining the range of a flight relies on knowing accurate weights to establish the required fuel. Unlike freight carriers which can obtain accurate payload weight data, airline operations are reliant on estimating the passenger payload from standard weights from regulators or establish their own estimations from surveys of passengers. With the average person getting heavier and the obesity prevalence varying from region to region, the use of standard weights can lead to either over or under estimations of the fuel necessary for a particular range requirement.

Fig. 5a, b and c presents the range of the aircraft for various altitudes (flight levels, FL) concerning different obesity scenarios, additional information relating to the passenger payload (W_p) and fuel weight (W_f). These ranges correspond to the maximum possible distance travelled for the payload and fuel combination for MTOW in each scenario. A common trend is that, as the obesity prevalence increases, the payload increases resulting in less available weight for fuel, consequently reducing the possible range. For the three aircraft, the difference between a higher and lower altitude is greater with lower obesity percentages compared to higher

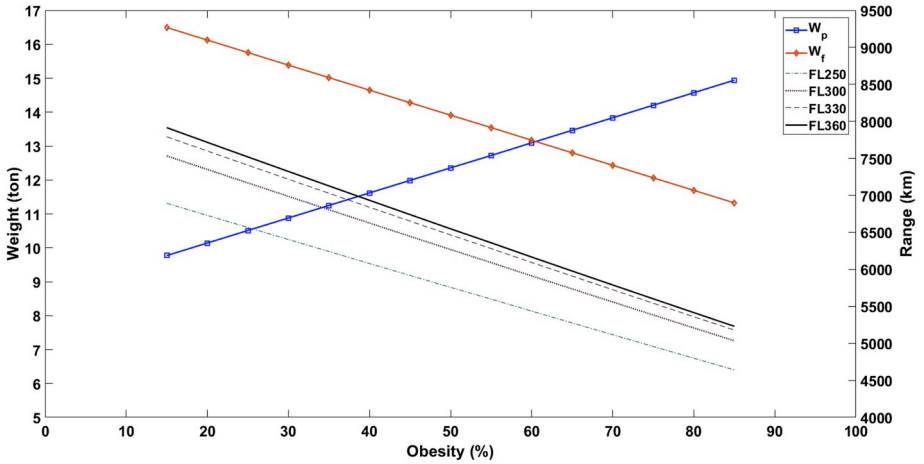

Fig. 5a. Maximum possible range at various altitudes for an A320, with MTOW for specified passenger payload and fuel weight combinations, over different obesity prevalence.

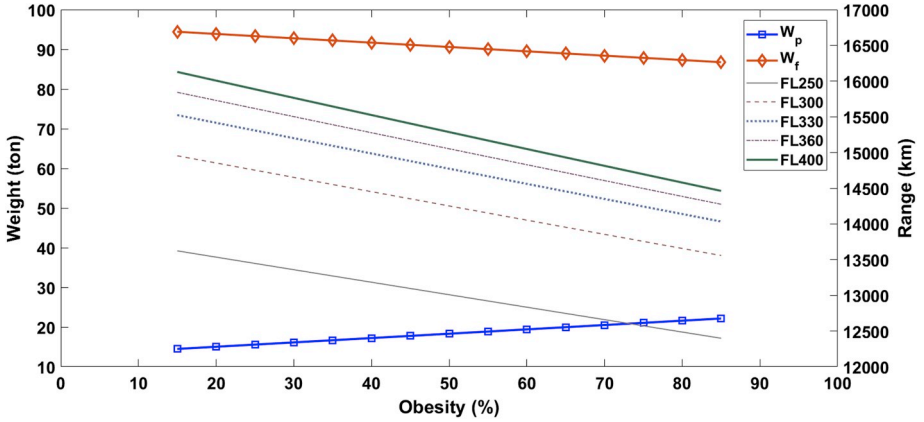

Fig. 5b. Maximum possible range at various altitudes for an A330-200, with MTOW for specified passenger payload and fuel weight combinations over, different obesity prevalence.

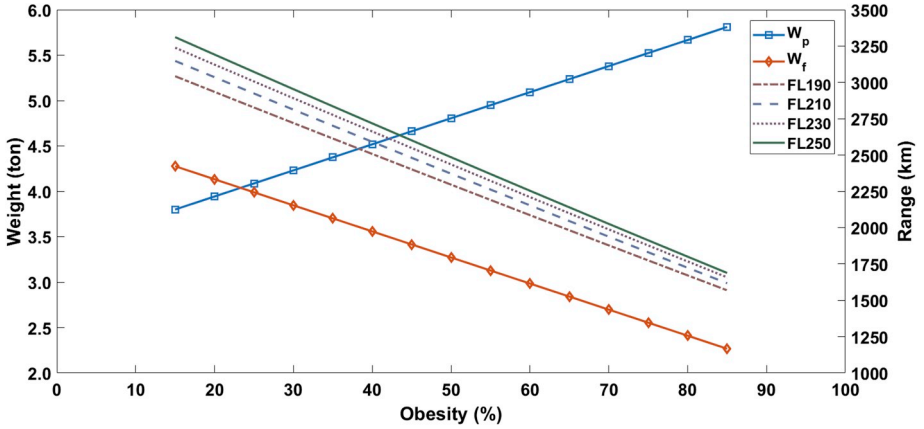

Fig. 5c. Maximum possible range at various altitudes for an ATR-72, with MTOW for specified passenger payload and fuel weight combinations over, different obesity prevalence.

scenarios. This would indicate that if a pilot has a flight plan for an assigned altitude range combination and decides to fly at a lower altitude, there will be less range as a consequence; nevertheless, it is common practice to request higher altitudes. It is interesting to note that at an obesity level of approximately 60% the passenger payload weight equals the fuel weight (Fig. 5a). The same point

Table 8
Comparison of maximum range possible for the three types of aircraft between key aviation regulators at MTOW with a passenger fuel combination.

Regulator	Passenger Payload (kg)	Fuel Weight (kg)	Maximum Range (km)
A320, FL360, Mach = 0.79			
ICAO	14,400	11,865	5684
FAA	14,040	12,225	5502
EASA	15,894	10,371	4756
CAA UK	14,220	12,045	5593
A330-200, FL360, Mach = 0.82			
ICAO	21,360	87,570	14,437
FAA	21,093	87,837	14,491
EASA	23,576	85,354	13,993
CAA UK	21,093	87,837	14,491
ATR-72, FL250, Mach = 0.42			
ICAO	5600	2477	1852
FAA	5460	2617	1962
EASA	6181	1896	1402
CAA UK	5530	2547	1907

occurs after the 20% obesity level for the ATR 72 (Fig. 5c). There is no point where this crossover occurs on the A330-200 aircraft (Fig. 5b). The A330-200 caters for long-range distances, thus requiring greater capacity for fuel (per weight) compared to payload for maximum possible range. For comparison, the maximum possible range for each aircraft with the standard passenger weight related to the four regulators is shown in Table 8. As shown in Fig. 2, the regulatory standard weights are higher than the average weights of many countries. When examining the aircraft ranges from Table 8 to the corresponding figures in Fig. 5, the range capabilities of the aircraft are conservative. Under regulatory standards, the aircraft show a lower range potential equivalent to a payload with an obesity prevalence of greater than 80% for the turbofan and greater than 70% for the turboprop.

3.4. Climb

In most flights, the aircraft follows a step climb procedure. In this situation, the aircraft will fly to an assigned altitude where it may level off. Then after some time, the air traffic controllers will indicate to the pilot to change altitude and speed, resulting in many potential flight paths from that point onward. This paper adopts a simplified approach by considering the aircraft follows a continuous climb path between take-off and cruise altitude.

Fig. 6 present the time to climb and rate of climb for two obesity scenarios (15% and 85%) for the three aircraft types considered herein. Only the two extreme scenarios are presented as the variation of the rate of climb and time to climb is small for any other cases. As expected, the general trend that is shown in Fig. 6 illustrates that as obesity increases the longer the aircraft will take to climb to any altitude. Similarly, the lighter the aircraft the higher rate of climb the aircraft can achieve. As an example, an A320 will take 16 min to climb to an altitude of 36,000 ft for the 15% obesity case, whereas this time increases to 19 min for the 85% obesity scenario.

Similarly, the A330-200 will take 25 min for an aircraft with 15% obesity and 29 min with 85%. Compared to the turbofan aircraft the ATR-72 generally flies at lower altitudes. Assuming a climb up to 25,000 ft, the ATR-72 will take 23 min and 32 min for the for 15% and 85 obesity cases, respectively. There is an evident greater impact of the passengers' weight change on the climb performance of the turboprop aircraft. In other words, results show that the effect of payload weight on the rate of climb and time to climb become less pronounced with the size and gross weight of an aircraft.

Data from the flight between SIN-MLE showed a time of 33 min to climb to FL360 corresponding to 2.7 tonnes of fuel. The model developed in this paper calculated that it would take 25 min and 2.8 tonnes of fuel to achieve the same flight level. The discrepancy in the

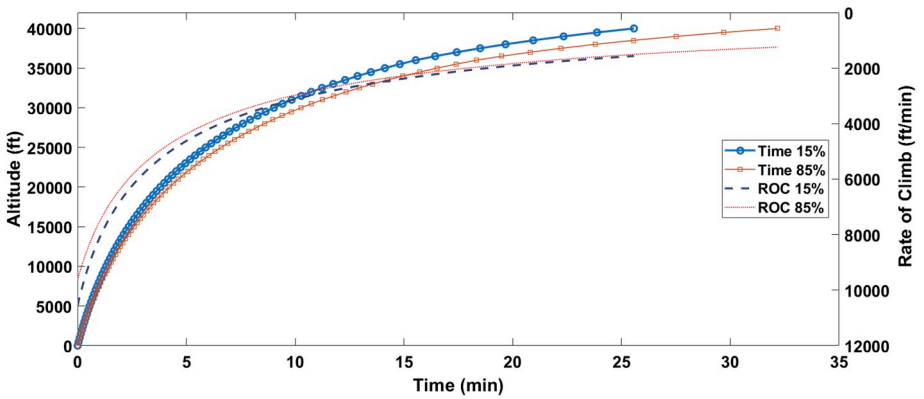

Fig. 6a. A320 Time to Climb and Rate of Climb for 15% and 85% obesity, considering a fuel weight for 3,000 km range.

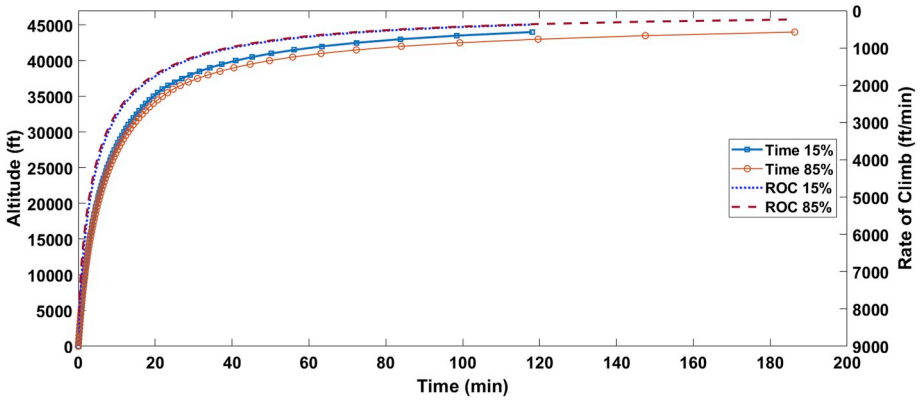

Fig. 6b. A330-200 Time to Climb and Rate of Climb for 15% and 85% obesity considering a fuel weight for 7,500 km range.

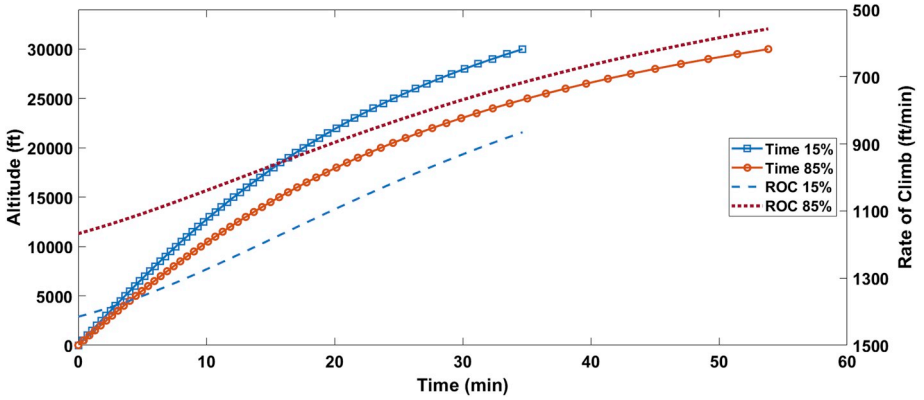

Fig. 6c. ATR 72 Time to Climb and Rate of Climb for 15% and 85% obesity considering a fuel weight for 700 km range.

time can be caused by the model considering a continuous climb profile while it is highly likely that the aforementioned flight experienced a step climb. Furthermore, the difference in the higher fuel for the model can also be attributed to the fact the ICAO Engine Databank fuel flow data is tested under a thrust condition of 85% maximum thrust. The SIN-MLE flight may have had a different power setting or other unknown aircraft characteristics (e.g., different engine model) that would likely lead to lower fuel consumption. Nevertheless, the calculated performance parameters are within expected values demonstrating the robustness of the model developed in this paper.

3.5. Take-off

The take-off phase is probably the most sensitive to the uncertainty around passengers weight as any deviation from the calculations made by pilots can lead to an exceedance of the required take-off distance. It is therefore of crucial importance pilots have the accurate aircraft weight to determine the correct take-off performance characteristics of their aircraft for a particular flight condition. To ensure a safe departure the upper limit of MTOW should not be exceeded. At the MTOW the model estimates that the A320, A330-200 and ATR-72 utilise 2,146 m, 2,793 m and 1,689 m of runway respectively. Using the same take-off weight for the A320 operating the SIN-MLE flight (i.e. 73,616 kg) the model predicted a take-off distance of 1,730 m, which is not very far from the value obtained from the Airbus A320 handbook (i.e. 1,800 m). For the ATR-72 aircraft, both the example provided in Filippone (2012) and the results obtained from this model pled to identical take-off distances (1,600 m) considering a take-off weight of 22,616 kg. These results demonstrate the accuracy of the model used in this paper.

Fig. 7a, b and c illustrates the take-off distance required for different obesity prevalence situations and selected ranges. Both the A320 and ATR-72 aircraft have relatively close take-off distances for different range scenarios, whereas the A330-200 has a relatively wider variation of take-off distance for across the considered range scenarios. Another point is that comparing the different range scenarios for the smaller aircraft shows that obesity prevalence has a greater effect when comparing the take-off distance for the two extreme obesity cases, i.e., 15% and 85% of obesity prevalence. The increase in the take-off distance can be as high as 300 m for the ATR-72 considering a target range of 1,000 km. For the A330-200 operating in High Income Western Countries [59.67% ± 3.6], and considering a range of 12,500 m, the calculated take-off distance is 2,400 m. Comparing a region consisting of lower obesity, such as Sub-Saharan Africa [28.21 ± 8.4], for a similar range the same aircraft would only use 2,300 m of tarmac. This difference is approximately 100 m for close to 30% change in payload due to obesity. On high capacity, short haul routes, e.g. 2,500 km, in high population density centre in East and South East Asia [57.82% ± 12.1] or High Income Asia Pacific [61.31% ± 5.6], the same

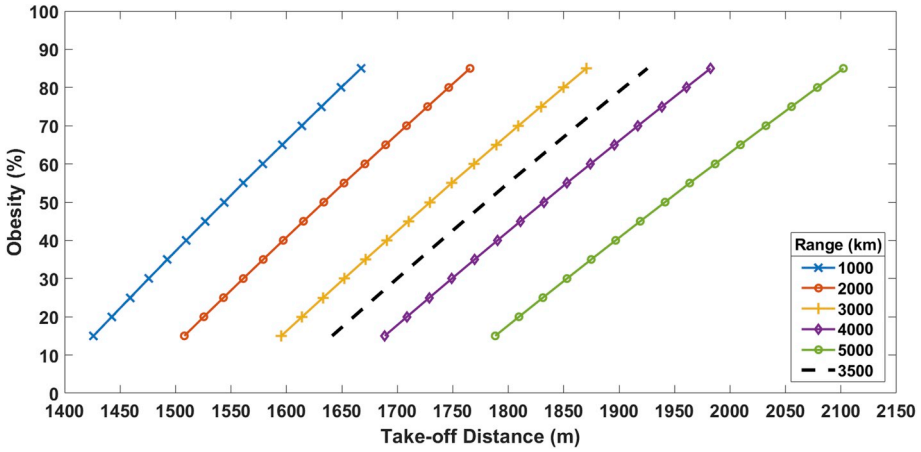

Fig. 7a. A320 Take-off distance vs obesity prevalence for various ranges at FL360.

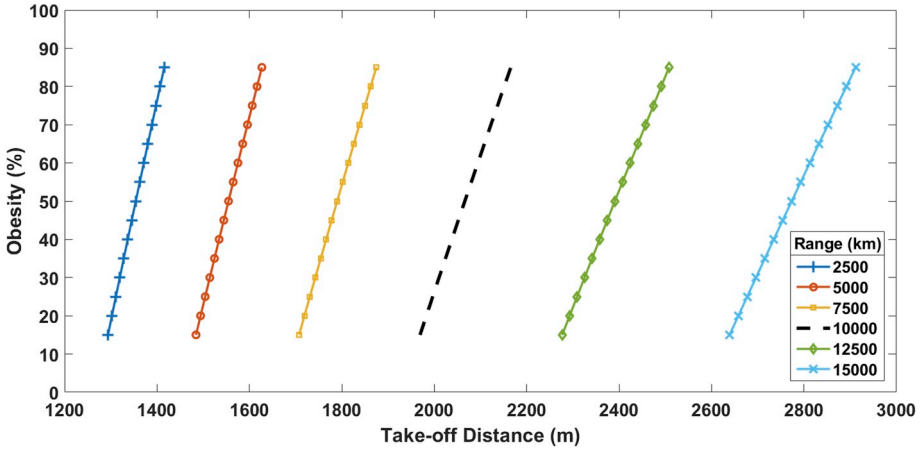

Fig. 7b. A330-200 Take-off distance vs obesity prevalence for various ranges at FL360.

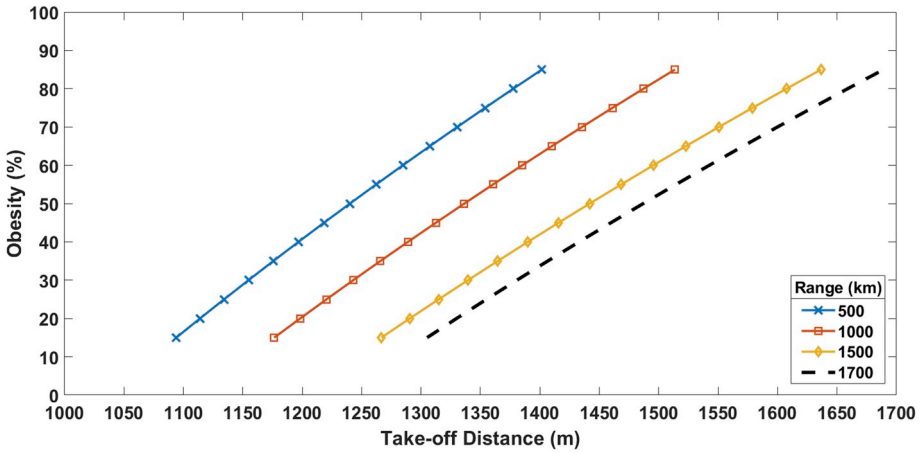

Fig. 7c. ATR-72 Take-off distance vs Obesity for various ranges at FL250.

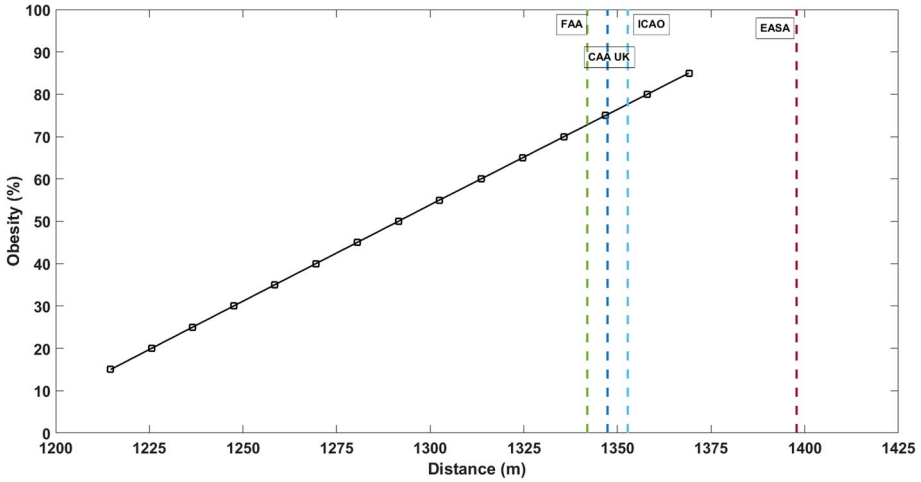

Fig. 8a. The effect different obesity levels have on the A320 landing distance. Vertical lines represent the landing distances as per the requirements set by the corresponding regulators.

aircraft utilising only 1,370 m of tarmac. However, using standard passenger weights the aircraft will use 1,400 m or runway for the same range.

3.6. Landing

From a performance perspective, ideal aircraft operations would see an aircraft consume the exact amount of fuel predicted for the flight, leaving residual fuel for taxing purposes. The model considered in this paper assumes that the aircraft will arrive at the destination with zero fuel on-board, allowing for the only variable to be passenger payload weight when determining the landing distance. Fig. 8a, b and c illustrates the landing distance for the A320, A330-200 and ATR-72 aircraft as a function of obesity prevalence respectively. Within each subfigure, the landing distances determined based on the requirements set by four regulators (i.e., FAA, ICAO, CAA UK and EASA) are shown as vertical lines. All these distances are shown for a zero-fuel weight condition of the aircraft. It is evident that the standard weights issued by regulators provide a conservative landing distance, as all four regulators' landing distances lie above an obesity equivalent level of 70%. Current global average obesity is close to 53% and is likely to reach 70% in the near future according to forecasts, thus narrowing the safety margin for the calculation of landing distances.

Landing distance is heavily influenced by the weight of the aircraft. Manufacturers provide a maximum landing weight of aircraft to prevent structural damage on touch down, including landing gear. This weight incorporates the maximum difference of fuel weight not spent during a flight for any zero-fuel weight. In an emergency during the early phases of flight, the aircraft would dump fuel to reach this weight. At maximum landing weight, the model predicts that the A320, A330-200 and ATR-72 utilise 1,439 m, 1,744 m and 1,148 m of runway respectively. Comparatively, the Airbus reference handbooks for the A320 and A330-200 show approximate

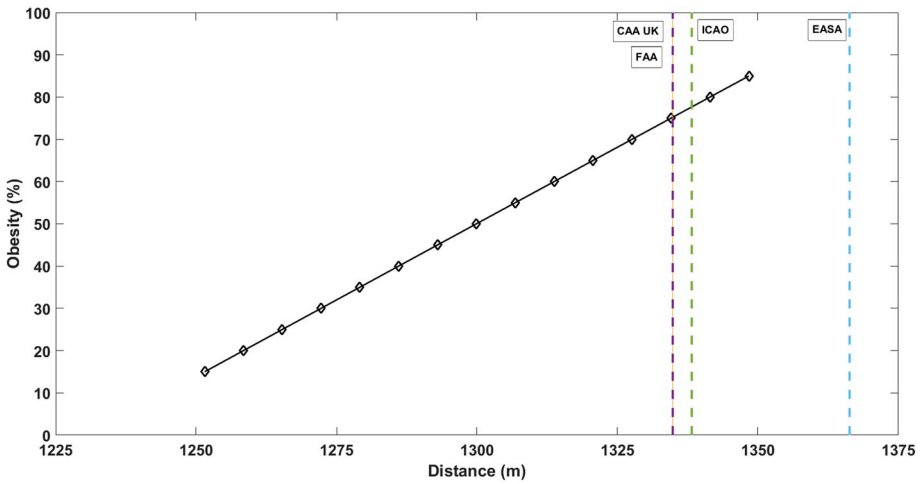

Fig. 8b. The effect different obesity levels have on the A330-200 landing distance. Vertical lines represent the landing distances as per the requirements set by the corresponding regulators.

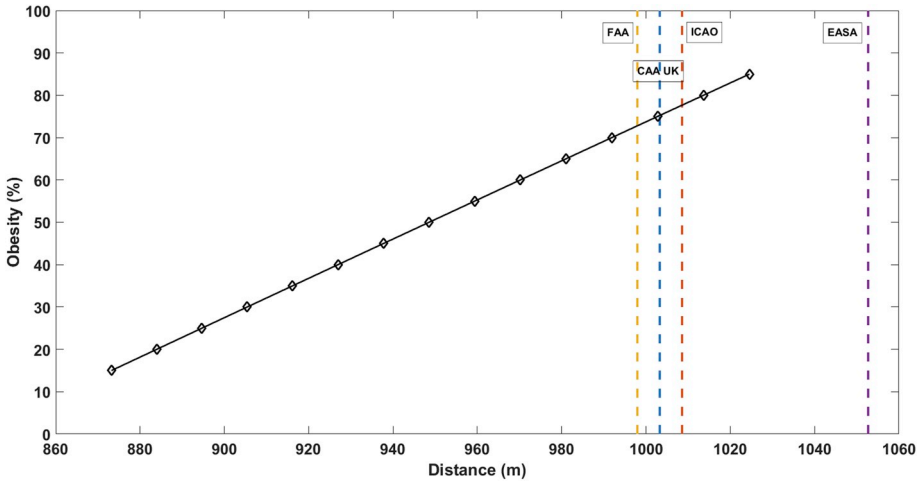

Fig. 8c. The effect different obesity levels have on the ATR 72 landing distance. Vertical lines represent the landing distances as per the requirements set by the corresponding regulators.

landing distance value of 1,400 m and 1,700 m respectively. These distances are computed based on standard passenger weights. However, and as seen before, different geographical regions may lead to significant deviations on the standard weight, thus resulting in deviation in calculated landing distances. This limitation may pose a serious operational risk for airports with relatively short runways and/or when other external factors may also have a concomitant detrimental effect on the aircraft performance, such as environmental temperature, condition of the runway pavement (e.g. wet vs dry), altitude of the airport, etc. For example, an A320 operated by an airline in South Asia [24.62% ± 3.5] is going to utilise 1,230 m of runway, compared to 1,310 m necessary for the very same aircraft and total number of passengers in a High Income Western country [59.67% ± 3.6].

3.7. Fuel and emissions

Knowing the correct amount of fuel needed for a flight is critical as fuel cost is a significant expenditure to an airline. However, the exact amount of fuel can only be calculated once the weights for both passengers and cargo are known for a given flight. The paradox is that only the cargo is weighed before boarding, whereas the passengers' weights are estimated from the standards adopted by the operator. Not knowing the correct weight of passengers can lead to excess fuel weight being carried during a flight or in the worse circumstance, not enough fuel.

Fig. 9a, b and c presents the cost and emissions associated with the fuel used for three aircraft flight scenarios that are presented in Table 6. In all aircraft cases, the cost of fuel and emissions rises with the prevalence of obesity due to the extra fuel required to transport the increased passenger weight. For the sake of an example, and considering the A330-200 with a range of 7,500 km, for every 5% increment of obesity added to the passenger payload, an additional 122.2 kg of fuel is required, emitting 362.5 kg of extra emissions at the cost of $92.25USD; an A320 travelling 3,000 km will need 54.8 kg of fuel, emitting 95.4 kg of emissions at an additional cost of $41.37USD; the ATR-72 travelling 700 km will carry 6.77 kg of fuel which will emit 15.3 kg of emissions and cost $5.11USD. However, for the extreme 85% obesity prevalence case the change in the fuel cost compared to an aircraft carrying a

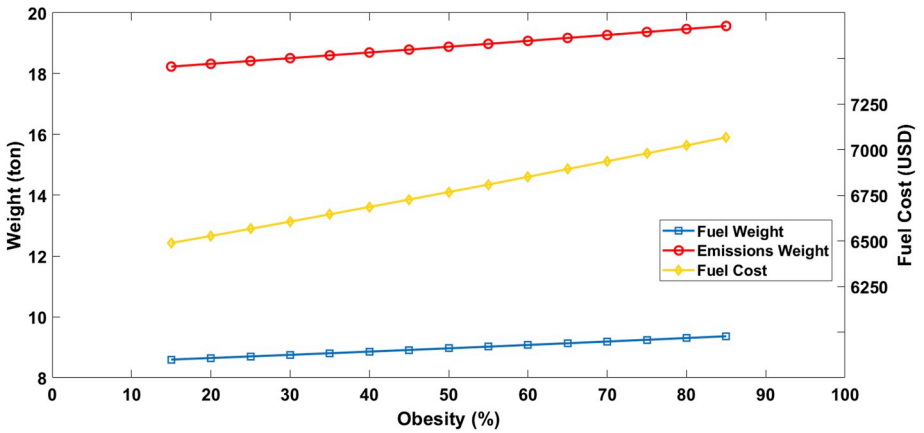

Fig. 9a. A320 fuel cost and emissions with fuel weight as a function of obesity prevalence (considering a range of 3,000 km).

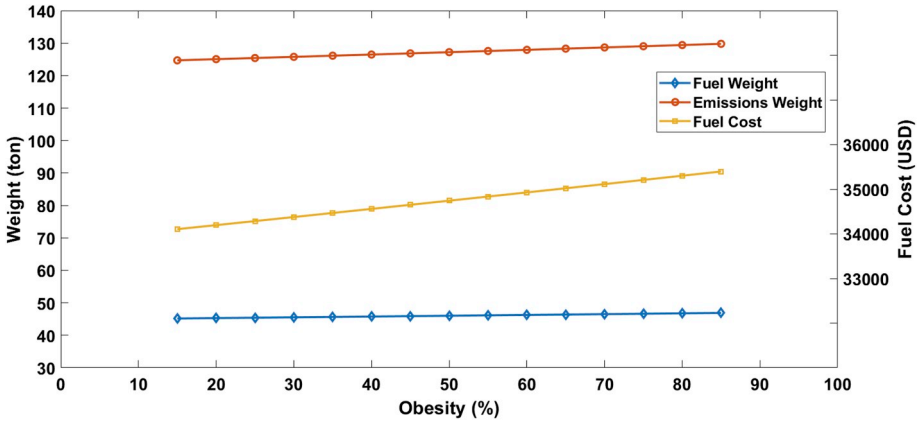

Fig. 9b. A330-200 fuel cost and emissions with fuel weight as a function of obesity prevalence (considering a range of 7,500 km).

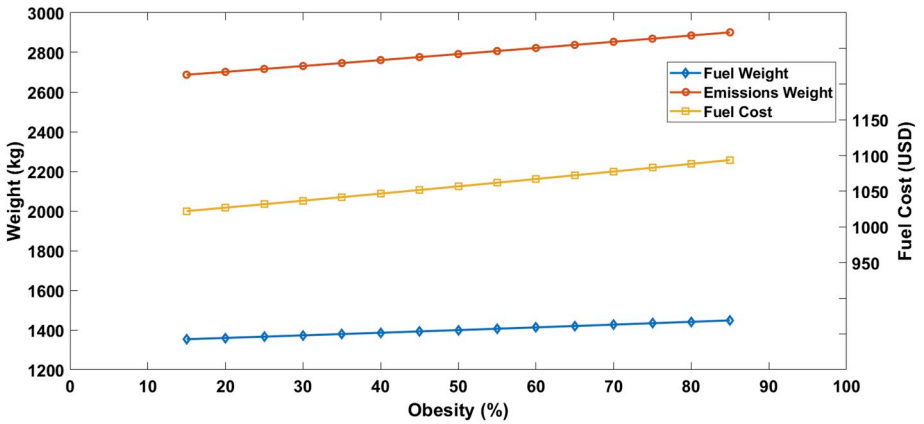

Fig. 9c. ATR72 fuel cost and emissions with fuel weight as a function of obesity prevalence (considering a range of 700 km).

passenger payload based on ICAO standard weights is 1.6% for the A320 and 0.5% for both the A330-200 and ATR-72. Though these percentages are small in absolute terms, it should be noted the financial impact in the long run is considerable, particularly for long range operations. This stresses the need for airlines to use accurate passenger weights instead of estimations based on standards as a means to save on fuel. Looking at Fig. 9a, if an A320 were to operate for an airline in sub Saharan Africa [28.21% ± 8.4] the airline would spend close to $6,600USD, while in other nations such as those in Oceania [71.81% ± 10.1] may spend up to $6,900USD for a similar distance. These values represent significant savings when compared against the fuel cost corresponding to the standard weights based on ICAO or EASA regulations, respectively $6,955USD and $7,135USD.

Park and O'Kelly (2014) determined that an A330-200 will use 43 tonnes of fuel to fly an average trip distance of 6,315 km, which contrasts with 33 tonnes obtained from the model used in this paper. Similarly, Yin et al. (2015) showed that a 9,260 km flight carried out by an A330-200 used 64 tonnes of fuel compared to 51 tonnes derived from the model in this paper. Their methods involved aggregating yearly fuel consumption and flight distances to provide flight characteristic estimates. It is noted that there a difference between the results of Park and O'Kelly (2014) and Yin et al. (2015) to those calculated using the model in this paper. These differences can be attributed unstated aircraft weights, the engine model or other parameters that can produce conservative results.

4. Conclusions

Overweight and obesity are placing a strain on society as well as industry at a global scale. The effects of passenger weight in the transport sector suffer from a lack of interest from key stakeholders, particularly with the associated safety, operational and financial implications. The contribution of this paper is in addressing this knowledge gap by analysing the changes in aircraft performance characteristics due to growing passenger weight. The resultant findings clearly show how obesity affects main aircraft performance parameters. From a safety and operational perspective, the results show that deviations from the average passenger weight (average passenger weight is stipulated by regulators) owing to different obesity prevalence rates can significantly compromise safety margins. This limitation is particularly evident for higher obesity prevalence rates which are in line with forecasts of obesity prevalence in the near future. Geographical factors potentially also play a role in the accuracy of calculated performance characteristics of different types of aircraft as distinct regions around the world have significantly different obesity rates. From an economics perspective, the

results obtained in this paper illustrate that the majority of the nations around the world are overestimating the standard weights of passengers, which represent unnecessary fuel costs to airlines as well as increased pollutant emissions. Overall, this paper has demonstrated the need for regulators to issue standards with updated passenger weights in line with current demographic trends, thereby resulting in more accurate flight performance calculations regardless of the operators' geographical context. Alternatively, a direct measuring of passenger weight prior to boarding would be an effective measure to reduce uncertainty around this parameter, though this procedure still requires public acceptance due to privacy issues.

Funding

The Authors did not receive any specific funding for this work.

Appendix A. Aircraft Range during Cruise

The lift coefficient is calculated using an estimated take-off weight (in this case, MTOW) and the velocity at altitude (Eq. (A1)). Where W is aircraft weight, S is wing area, ρ is air density as altitude and V is velocity. The drag coefficient and lift to drag ratio is then calculated using Eq. (A2) and Eq. (A3) respectively. Where k is the induced drag factor and C_{Do} is the zero-drag value.

$$C_L = \frac{2W}{\rho S(V^2)} \tag{A1}$$

$$C_D = C_{Do} + kC_L^2 \tag{A2}$$

$$E = \left(\frac{C_L}{C_D}\right) \tag{A3}$$

Since drag is equal to thrust during cruise, the available thrust can be obtained by Eq. (A4).

$$D \approx T = \Delta T_o \left(\frac{\rho}{\rho_o}\right)^i \left(\frac{M}{M_o}\right)^{M_{exp}} \tag{A4}$$

Where T is available thrust, T_o is the maximum thrust produced by the engine at sea level; i is a factor determined by altitude (below 11,000 m $i = 1$, above 11,000 m $i = 1.2$); Δ is the throttle setting, ρ is the air density at the given altitude and ρ_o is the corresponding sea level value. M_o is a reference Mach number until which T can be kept in the maximum value for that altitude. $M_{\exp}$ is the thrust versus speed dependence factor, this being $M_{\exp} = 0.75$ for the turbofan and $M_{\exp} = 1$ for the turboprop. $M_{\exp} = 0$ corresponds to the turbojet. A value of $M_{\exp} = 1$ means that the by-pass ratio is very high to such extent that is the engines operation can be compared to that of a propeller driven engine. The model presented assumes a known ZFW, calculated from the OWE plus the calculated payload weight based on BMI prevalence.

The range models described stem from the Specific Range (SR), Eq. (A5a) and Eq. (A5b) for turbofan and turboprop aircraft respectively. SR is the distance flown divided by the amount of fuel consumed. Then by integrating the SR over the weight of the aircraft, and by multiplying both the numerator and denominator by the lift force, the resultant formula is the Breguet range equation (Eq. (A5c)).

$$SR_{TF} = \frac{dx}{dW} = \frac{Vdt}{cTdt} = \frac{V}{cD} \tag{A5a}$$

$$SR_{TP} = \frac{dx}{dW} = \frac{Vdt}{cPdt} = \frac{\eta Vdt}{cTVdt} = \frac{\eta}{cD} \tag{A5b}$$

$$X = \left(\frac{E}{c}\right) \int_{w_1}^{w_2} V \frac{dW}{W} \tag{A5c}$$

The maximum lift to drag coefficient is given by Eq. (A6). This parameter is common in both turbofan aircraft (Eq. (20)) and turboprop aircraft (Eq. (21)).

$$E_{max} = \frac{1}{\sqrt{4kC_{Do}}} \tag{A6}$$

The reported fuel flows in the ICAO databank are presented for each phase of the landing/take-off cycle and does not provide cruise fuel flow data. Thus, trust specific fuel consumption (TSFC) is needed to be calculated for the cruise segment. TSFC is dependent on Mach, altitude and engine by-pass ratio. Howe (2000) presents a method for calculating TSFC for a turbofan based on Mach, altitude and engine by-pass ratio (Eq. (A7)). The values of TSFC in Table 5 are calculated from Eq. (A7) for an altitude of 36,000 ft and a Mach listed in Table 6 for each turbofan aircraft for the respective scenario. The PSFC for the turboprop aircraft is given by Avions de Transport Regional (2001) and is shown in Table 5.

$$c = c'(1 - 0.15\beta^{0.65})(1 + 0.28(1 + 0.063\beta^2)M)\left(\frac{\rho}{\rho o}\right)^{0.06} \tag{A7}$$

Where c' is approximate to 20 mg $N^{-1}s^{-1}$ (Howe, 2000), β is the by-pass ratio, M is the Mach number.

Appendix B. Climb Calculations

The rate of climb (ROC) characteristics are established by determining the take-off weight from a calculated zeta value for a cruise situation. Velocity and thrust for the climb phase are calculated using Eq. (B1) and Eq. (A4). The Mach number associated with V_{ROC} for a given altitude is used in Eq. (A4) to determine the thrust.

$$V_{ROC} = \left[\left(\frac{T}{3\rho C_{Do} S} \right) \left(1 + \sqrt{1 + \left(\frac{3}{\left[\frac{1}{\sqrt{4kC_{Do}}} \left(\frac{T}{W} \right) \right]^2} \right)} \right) \right]^{\frac{1}{2}} \tag{B1}$$

The climb angle is determined by Eq. (B2) (Sadraey, 2017). Where T is the thrust, k is the induced drag coefficient and W is the aircraft weight. Both the Velocity and climb angle are need to follow to procedure in Sadraey (2017).

$$\gamma_{ROC} = \sin^{-1}\left[\frac{T - D}{W} \right] = \sin^{-1}\left[\frac{T}{W} - \frac{\rho V_{ROC}^2 S C_{Do}}{2W} - \frac{2kW}{\rho S V_{ROC}^2} \right] \tag{B2}$$

Appendix C. Descent Calculations

The descent model determines the rate of descent (ROD) for a given landing weight and considering a given payload of obesity prevalence amongst passengers. Typical descent for transport aircraft involves some level of thrust to maintain airspeed. Thus, the model presented also assumes that during the descent phase thrust is being produced. The descent profile for this model is assumed to be a continuous descent flight path with constant deceleration from cruise speed to landing speed and constant descent angle.

For this particular scenario, the known quantities of the initial condition, V_i is equal to cruise velocity, and cruise altitude is known. The final condition consists of a V_f being equal to the approach velocity for landing with a final altitude equivalent to the clearance height mentioned in Section 2.5.3. For the purpose of the results presented in this paper, a 2° flight path angle was considered. The air distance was determined by using Eq. (C1). Where h_i is the initial altitude, h_{i-1} is a lower altitude. Deceleration is obtained from Eq. (C2) which is applicable to a particular phase of descent ranging from an initial altitude and corresponding speed (V_i) to a final altitude and speed (V_j), where a_x is the acceleration along the flight path, and X is the distance along the flight path.

$$X = \sqrt{{h_i}^2 + \left(\frac{h_{i-1}}{\tan \gamma_{desc}} \right)^2} \tag{C1}$$

$$a_x = \frac{V_j^2 - V_i^2}{2(X)} \tag{C2}$$

Then, using Eq. (C3), the speed at a given stage of altitude is determined. The lift component is calculated (Eq. (C4)) followed by the drag (Eq. (C5)).

$$V_{h_f} = \sqrt{V_i^2 + 2a\Delta h} \tag{C3}$$

$$L_{desc} = W\cos(\gamma_{desc}) \tag{C4}$$

$$D_{desc} = \frac{1}{2}\rho V^2 S(C_{Do} + kC_L^2) \tag{C5}$$

The required thrust to maintain airspeed during descent is calculated from Eq. (C6). Then using Eq. (17a) and Eq. (17b), the rate of descent is calculated. Note that a negative ROC indicates descending aircraft.

$$T_{R_{desc}} = D_{desc} - W\sin(\gamma_{desc}) + m_{ac} a_x \tag{C6}$$

Appendix D. Take-off and Landing Calculations

An aircraft's take-off performance relies on knowing the take-off weight and air ambient condition (assumed to be International Standard Atmosphere). The weight can only be known once the flight range is determined. In the model presented, a take-off weight is chosen by selecting the appropriate zeta-range combination. Rearranging Eqs. (15)–(16) from section 2.5.1 for the fuel fraction yields Eq. (D1).

$$\xi_i = \frac{B}{BkC_L E + E} \tag{D1}$$

where

$B = 2E_{max} \tan\left(\frac{X}{A_i}\right)$, i *is TF or TP*, and: $A_{TF} = \frac{2VE_{max}}{c}$ or $A_{TP} = \frac{2\xi E_{max}}{c}$.

The resultant take-off weight is then calculated using the zeta value and a selected ZFW associated with the obesity passenger payload using to Eq. (11) in Section 2.3.2. The manoeuvre speeds are determined by using the take-off weight and the stall speed (Eq. (36)). The coefficients of drag (C_{DLO}) and lift (C_{LLO}) at lift-off are determined using the related speeds. The ground roll distance is then determined from Eq. (D2).

$$X_{grd} = \left(\frac{1}{2B}\right)\ln\left(\frac{B}{B + AV_1^2}\right) \tag{D2}$$

where,

$A = \left(\frac{T_o}{\left(\frac{W_{lo}}{g}\right)}\right) - \mu g$; $B = \frac{-\rho S}{2\left(\frac{C_{LLO}}{g}\right)(1 - C_{DLO} - \mu C_{LLO})}$.Where V_1 is the speed at the end of the ground roll, T_o is the net thrust, W_{to} is the take-off weight, g is gravity, ρ is the air density, S is the wing area, μ is the strip surface rolling friction coefficient, and C_{iLO} is the lift-off coefficient.

Sadraey (2017) comments that the calculation to determine the distance travelled during the rotation phase is complex and suggests that using the V_{LO} multiplied by the time taken to rotate (Eq. (D3)) is a reasonable approximation. For transport aircraft, a timeframe of 3–6 s is recommended, hence for this study a rotation time of 3 s was considered.

$$X_{rot} = t_{rot} V_{LO} \tag{D3}$$

The airborne distance covered is determined by using Eq. (D4) and Eq. (D5). Where T_{ab} is approximately 90% of T_o (Sadraey, 2017), X_{ab} is the distance travelled on the ground, X'_{ab} is the distance travelled along the flight path, h_o (50 ft = 15.24 m) is the clearance height and D_{ab} is the drag during the airborne phase.

$$X'_{air} = \left(\frac{W}{T_{ab} - D_{ab}}\right)\left[\frac{(V_2^2 - V_{LO}^2)}{2g} + h_o\right] \tag{D4}$$

$$X_{air} = \sqrt{X'^2_{ab} - h_o^2} \tag{D5}$$

The landing calculations in this model look at determining the field length for a given landing weight assumed to be the ZFW, for a given payload of obesity prevalence. The process of calculating the field length for landing is the reverse process of the take-off calculations. There are three phases to the landing; the approach, flare and ground roll. The same method is used to determine the specific landing speed as in the take-off procedure. The manoeuvre speeds are determined from Eq. (15). The coefficients of drag (C_{DLgrd}) and lift (C_{LLgrd}) at the point of landing are determined using the related velocities.

The airborne distance covered is determined by using Eq. (D4) and Eq. (D5); however, in this case T_{ab} is zero since there is no thrust being produced. The touchdown follows the same method as the rotation phase (Eq. (D5)). The ground roll is determined by Eq. (D6).

$$X_{L_{grd}} = \left(-\frac{W}{\rho S g (C_{D_{Lgrd}} - \mu C_{L_{Lgrd}})}\right)\ln\left[\frac{\left(\left(\frac{1}{w}\right)(T_{rev} + F_B) + \mu\right)}{\left(\frac{1}{W}\right)(T_{rev} + F_B) + \mu\left(\frac{K_L^2}{C_{Lmax}}\right)(C_{D_{Lgrd}} - \mu C_{L_{Lgrd}})}\right] \tag{D6}$$

Where T_{rev} is the thrust produced from the thrust reverser (assumed 50% of T_o), K_L is the landing speed factor, and F_B is the force due to braking.

References

Ahmadpour, N., Lindgaard, G., Robert, J.-M., Pownall, B., 2014. The thematic structure of passenger comfort experience and its relationship to the context features in the aircraft cabin. Ergonomics 57 (6), 801–815.

Airbus, 2014. A330 Aircraft Characteristics Airport and Maintenance Planning, Airbus S.A.S, Blagnac Cedex, France.

Airbus, 2015. A320 Aircraft Characteristics Airport and Maintenance Planning, Airbus S.A.S, Blagnac Cedex, France.

Ananthapavan, J., Sacks, G., Moodie, M., Carter, R., 2014. Economics of obesity—learning from the past to contribute to a better future. Int. J. Environ. Res. Public Health 11 (4), 4007–4025.

Arul, S.G., 2014. Methodologies to monetize the variations in load factor and GHG emissions per passenger-mile of airlines. Transport. Res. Transport Environ. 32, 411–420. https://doi.org/10.1016/j.trd.2014.08.018.

ATR DC/E, 2014. ATR Family - Propelling the Next Connection. Blagnac cedex, France.

ATSB, 2014. Loading Issue Involving a Boeing 737, VH-VZO at Canberra Airport, ACT on 9 May 2014. Australian Transport Accident Bureau, Canberra.

Avions de Transport Regional, 2001. ATR: The Optimum Choice for a Friendly Environment, *Avions de Transport Regional, Blagnac Cedex*.

Babikian, R., Lukachko, S.P., Waitz, I.A., 2002. The historical fuel efficiency characteristics of regional aircraft from technological, operational, and cost perspectives. J. Air Transp. Manag. 8 (6), 389–400.

Barclay, M., Harris, J., Everingham, J.-A., Kirsch, P., Arend, S., Shi, S., Kim, J., 2013. Factors Linked to the Well-Being of Fly-In-Fly-Out (FIFO) Workers. Sustainable Minerals Institute, University of Queensland, Brisbane. https://www.csrm.uq.edu.au/publications/factors-linked-to-the-well-being-of-fly-in-fly-out-fifo-workers.

Berdowski, Z., Broek-Serlé, F. N. v. d., Jetten, J.T., Kawabata, Y., Schoemaker, J.T., Versteegh, R., 2009. Survey on Standard Weights of Passengers and Baggage (Report No. EASA 2008.C.06/30800/R20090095/30800000/FBR/RLO). EASA, Cologne, Germany.

Bil, C., Hanlon, G., 2016. Influence of ethnicity on passenger standard weight. In: Paper Presented to 30th Congress of the International Council of the Aeronautical Sciences. ICAS 2016.

Bolton, B., 2004. Battle for the armrest reaches new heights: the air carriers access act and the issues surrounding the airlines' policy of requiring obese passengers to purchase additional tickets. J. Air Law Comm. 69, 803.

CASB, 1988. Aviation Occurrence Report, Arrow Air Inc. Douglas DC-8-63 N950JW, Gander International Airport, Newfoundland, 12 December 1985. Report Number

85-H50902, Canadian Accident Safety Board, Ottawa, Canada.
CDC, 2015. National Health And Nutrition Examination Survey (NHANES) 2013-2014, Centers for Disease Control and Prevention. https://wwwn.cdc.gov/nchs/nhanes/ContinuousNhanes/Default.aspx?BeginYear=2013.
Chaves, F.A.V., Silvestre, M.A.R., Gamboa, P.V., 2018. Preliminary development of an onboard weight and balance estimator for commercial aircraft. Aero. Sci. Technol. 72 (Suppl. C), 316–326.
Chèze, B., Gastineau, P., Chevallier, J., 2011. Forecasting world and regional aviation jet fuel demands to the mid-term (2025). Energy Policy 39 (9), 5147–5158.
Dalmau, R., Prats, X., 2015. Fuel and time savings by flying continuous cruise climbs: estimating the benefit pools for maximum range operations. Transport. Res. Transport Environ. 35, 62–71.
Dannenberg, A.L., Burton, D.C., Jackson, R.J., 2004. Economic and environmental costs of obesity: the impact on airlines. Am. J. Prev. Med. 27 (3), 264.
Eshelby, M.E., 2000. Aircraft Performance : Theory and Practice. AIAA ; Arnold, Reston, Va. : London.
Filippone, A., 2012. Advanced Aircraft Flight Performance. Cambridge University Press, Cambridge ; New York.
Finkelstein, E.A., Khavjou, O.A., Thompson, H., Trogdon, J.G., Pan, L., Sherry, B., Dietz, W., 2012. Obesity and severe obesity forecasts through 2030. Am. J. Prev. Med. 42 (6), 563–570.
Finucane, M.M., Stevens, G.A., Cowan, M.J., Danaei, G., Lin, J.K., Paciorek, C.J., Singh, G.M., Gutierrez, H.R., Lu, Y., Bahalim, A.N., 2011. National, regional, and global trends in body-mass index since 1980: systematic analysis of health examination surveys and epidemiological studies with 960 country-years and 9· 1 million participants. Lancet 377 (9765), 557–567.
Gritsch, M., Bil, C., Hanlon, G., 2017. Review of standard passenger and cabin luggage weight procedures. In: Proceedings of the 17th Australian International Aerospace Congress', Paper Presented to (AIAC 2017), Melbourne, Australia, 26 - 28 February 2017.
Hammond, R.A., Levine, R., 2010. The economic impact of obesity in the United States', *Diabetes, metabolic syndrome and obesity*. Targets Ther. 3, 285–295.
Hileman, J.I., Katz, J.B., Mantilla, J., Fleming, G., 2008. Payload fuel energy efficiency as a metric for aviation environmental performance. In: Paper Presented to Proceedings of the 26th International Congress of the Aeronautical Sciences.
Howe, D., 2000. Aircraft Conceptual Design Synthesis. Professional Engineering Pub, London.
IATA, 2018. *Jet Fuel Price Monitor*, International Air Travel Association. viewed 22/10 2018. https://www.iata.org/publications/economics/fuel-monitor/Pages/index.aspx.
International Civil Aviation Organisation, 2014. Methodology ICAO Carbon Calculator V7. International Civil Aviation Organisation, Montreal, Canada.
International Civil Aviation Organisation, 2017. ICAO Aircraft Engine Emissions Databank, Doc. 9646-AN-943. ICAO, Montreal.
Joyce, S.J., Tomlin, S.M., Somerford, P.J., Weeramanthri, T.S., 2013. Health behaviours and outcomes associated with fly-in fly-out and shift workers in Western Australia. Intern. Med. J. 43 (4), 440–444.
Kaivanto, K., Zhang, P., 2018. A fuel-payload ratio based flight-segmentation benchmark. Transport. Res. Transport Environ. 63, 548–559.
Khadilkar, H., Balakrishnan, H., 2012. Estimation of aircraft taxi fuel burn using flight data recorder archives. Transport. Res. Transport Environ. 17 (7), 532–537.
Küchemann, D., 1978. The Aerodynamic Design of Aircraft. Pergamon Press, Oxford.
Lobstein, T., 2015. Prevalence and costs of obesity. Medicine 43 (2), 77–79.
Mazraati, M., Alyousif, O.M., 2009. Aviation fuel demand modelling in OECD and developing countries: impacts of fuel efficiency. OPEC Energy Rev. 33 (1), 23–46. https://doi.org/10.1111/j.1753-0237.2009.00161.x.
McCormick, B.W., 1995. Aerodynamics, Aeronautics, and Flight Mechanics, second ed. edn. Wiley, New York.
Melis, D.J., Silva, J.M., Silvestre, M.A., Clothier, R., 2017. Characterisation of the anthropometric features of airline passenger and thier impact on fuel usage in the Australian domestic aviation sector. In: Paper Presented to 17th Australian Aerospace Congress, Melbourne, Australia, 26-28 February 2017.
Melis, D.J., Silva, J.M., Yeun, R.C.K., 2018. Impact of biometric and anthropometric characteristics of passengers on aircraft safety and performance. Transport Rev. 38 (5), 602–624.
Mylrea, R., 2009. A growing body of law: obesity, disability, and the airline industry. Tulane J. Int. Comp. Law 18, 207.
NCD Risk Factor Collaboration, 2016a. Adiposity - Data, 2016, edn. School of Public Health, Imperial College, London 10/06/2016. http://www.ncdrisc.org/d-adiposity.html.
NCD Risk Factor Collaboration, 2016b. Height - Data, 2016, edn. Scool of Health, Imperial Collage, London 10/06/2016. http://www.ncdrisc.org/d-height.html.
NCD Risk Factor Collaboration, 2016c. Trends in adult body-mass index in 200 countries from 1975 to 2014: a pooled analysis of 1698 population-based measurement studies with 7;2 million participants. Lancet 387 (10026), 1377–1396.
Nikoleris, T., Gupta, G., Kistler, M., 2011. Detailed estimation of fuel consumption and emissions during aircraft taxi operations at Dallas/Fort Worth International Airport. Transport. Res. Transport Environ. 16 (4), 302–308.
Niţă, M.F., 2008. Aircraft Design Studies Based on the ATR 72'. Hamburg University of Applied Sciences.
NTSB, 2004. Loss Of Pitch Control during Takeoff Air Midwest Flight 5481 Raytheon (Beechcraft) 1900D, N233YV Charlotte. *North Carolina*, National Transport Safety Board, Washington, D.C.
Park, Y., O'Kelly, M.E., 2014. Fuel burn rates of commercial passenger aircraft: variations by seat configuration and stage distance. J. Transp. Geogr. 41 (0), 137–147. https://doi.org/10.1016/j.jtrangeo.2014.08.017.
Patel, H., D'Cruz, M., 2017. Passenger-centric factors influencing the experience of aircraft comfort. Transport Rev. 1–18.
Roskam, J., 1985. Airplane Design, Part 1: Priliminary Sizing of Aircraft, fourth ed. DARcorporation, Lawrence, Kansas.
Sadraey, MHa, 2017. Aircraft Performance : an Engineering Approach. CRC Press, Taylor & Francis Group, Boca Raton, FL.
Slater, G.L., 2002. Adaptive improvement of aircraft climb performance for air traffic control applications. In: Paper Presented to Proceedings of the IEEE Internatinal Symposium on Intelligent Control, 30-30 Oct. 2002.
Small, J., Harris, C., 2012. Obesity and tourism: rights and responsibilities. Ann. Tourism Res. 39 (2), 686–707.
Soler, M., Olivares, A., Staffetti, E., Zapata, D., 2012. Framework for aircraft trajectory lanning toward an efficient air traffic management. J. Aircr. 49 (1), 341–348 (Jan).
Thomas, D.M., Weedermann, M., Fuemmeler, B.F., Martin, C.K., Dhurandhar, N.V., Bredlau, C., Heymsfield, S.B., Ravussin, E., Bouchard, C., 2014. Dynamic model predicting overweight, obesity, and extreme obesity prevalence trends. Obesity 22 (2), 590–597.
Tom, M., Fischbeck, P., Hendrickson, C., 2014. Excess passenger weight impacts on US transportation systems fuel use (1970–2010). J. Transport Health 1 (3), 153–164.
Turgut, ET, Cavcar, M., Usanmaz, O., Canarslanlar, A.O., Dogeroglu, T., Armutlu, K., Yay, O.D., 2014. Fuel flow analysis for the cruise phase of commercial aircraft on domestic routes. Aero. Sci. Technol. 37, 1–9.
Van Es, G., 2007. Analysis of Aircraft Weight and Balance Related Safety Occurrences. Nationaal Lucht- en Ruimtevaartlaboratorium, Amsterdam, The Netherlands.
Vasel, K., 2017. Lawmakers look to stop shrinking airplane seats. CNN Money Int. http://money.cnn.com/2017/03/10/pf/congress-airplane-seat-size-limit-legislation/index.html Retrieved from, 10-03-17.
Vink, P., van Mastrigt, S., 2011. The aircraft interior comfort experience of 10,032 passengers. In: paper Presented to Proceedings of the Human Factors and Ergonomics Society Annual Meeting.
Wang, Y., Lim, H., 2014. Epidemiology of obesity: the global situation. In: Integrative Weight Management. Springer, pp. 19–34.
WHO, 2016. Obesity Situation and Trends. World Health Organisation viewed 4/4/16 2016.
Yin, K-s, Dargusch, P., Halog, A., 2015. An analysis of the greenhouse gas emissions profile of airlines flying the Australian international market. J. Air Transp. Manag. 47, 218–229.